NOTE TO USERS

DALHOUSIE UNIVERSITY

To comply with the Canadian Privacy Act the National Library of Canada has requested that the following pages be removed from this copy of the thesis:

Preliminary Pages
- Examiners Signature Page
- Dalhousie Library Copyright Agreement

Appendices
- Copyright Releases (if applicable)

ANALYTICAL APPROACH OF THE TRANSIENT GREEN'S FUNCTION SOLUTION FOR THE LINEAR THREE-DIMENSIONAL WAVE-BODY INTERACTION PROBLEM

by

Aries Sulisetyono

Submitted in partial fulfillment of the

requirements for the degree of

DOCTOR OF PHILOSOPHY

Major Subject: Naval Architecture

at

DALHOUSIE UNIVERSITY

Halifax, Nova Scotia December 2004

Your file Votre référence
ISBN: 0-494-02122-5
Our file Notre référence
ISBN: 0-494-02122-5

Contents

List of Tables

List of Figures

List of Symbols and Abbreviations

a	non-dimensional frequency
a, b, c	coefficients of series
$\bar{a}, \bar{b}, \bar{c}$	a half of length, beam, and draft of ellipsoid
$\vec{A}$	control points
A	added mass coefficient in frequency domain
B	damping coefficient in frequency domain
C	hydrostatic restoring force in frequency domain
$\vec{d}, \vec{e}$	unit tangent vector
ET	the elapsed time
$\tilde{F}$	memory part of Green's function
$\tilde{F}_n$	normal of memory part of Green's function
F_{jk}^R	radiation forces
g	acceleration due to gravity
G	Green's function
G_0	impulsive part of Green's function
H	a half length to draft ratio
$H(t)$	heavside function of time
J	Jacobian

J_ω	Jacobian including weighting function
J_0	bessel function of zeroth order
K	wavenumber
K_{jk}^R	impulse response function
L_t	maximum time simulation
M_{ev}	total expansion order
M_1, M_2, M_3	total expansion orders of series
N	number of Gaussian points
n_x, n_y, n_z	unit normal vector
n_k	outward unit normal, $k = 1, 2, ..., 6$
$N(u), N(v)$	basis function of NURBS surface
ODE	ordinary differential equation
p	hydrodynamic pressure
P	field point
PSGf	power series of Greens function
$\bar{p}, \bar{q}$	degrees of basis function
q_k	body boundary condition
Q	source point
r	radius of the body
RMS	root mean square error
R.D	relative different
S_F	free-surface domain
S_B	body surface domain
S_∞	bounding surface at infinity
t	time

t_0	initial time
u, v	parameter function
U, V	non-uniform knot vectors
w	weighting function
$\vec{U}$	fluid velocity
$\vec{W}(u, v)$	position vector along the NURBS surface
$\vec{W}'(u, v)$	position vector along NURBS surface of the new body
x, y, z	cartesian co-ordinate system
X, Y, Z	location of control point
l_e, θ	parametric form of ellipsoid
$[G], [H]$	kernel matrix of the boundary integral
$\vec{\eta_k}$	six component vector of translation and rotation motions
η_1, η_2, η_3	surge, sway, and heave of translation motions
η_4, η_5, η_6	roll, pitch, and yaw of rotation motions
Ω	fluid domain
ϕ	velocity potential
ϕ_T	total velocity potential
ϕ_R	velocity potential due to wave radiated
ϕ_D	velocity potential due to wave diffracted
ϕ_I	velocity potential due to incident wave
ϕ_7	velocity potential due to scattering wave
ς	free-surface elevation
$\delta(t)$	delta function
$\frac{1}{r}$	rankine ring source
μ, β	non-dimensional of F functions

ϕ_e	equipotential surface
ρ	fluid density
$\lambda_{jk}\beta$	damping coefficient at zero time condition
μ_{jk}	infinite fluid added mass
ω	frequency
Δt	time-step size
$\Delta\beta$	time-range

Acknowledgements

I would like to express my sincere appreciations to my supervisor Professor R. Islam for his technical guidance and supervision during the development of this research work and also provided me with financial assistance. I wish to acknowledge the valuable advice given by my co-supervisor, Dr. M. Koksal, and I also would like to thank my thesis committe members, Professor J. Militzer and Professor M. Rahman for their suggestions and comments on my thesis work.

I gratefully acknowledge the Post Graduate of Marine Technology, Faculty of Ocean Engineering, Institut Teknologi Sepuluh Nopember Surabaya for providing the financial support through the Center Urge Project throughout my studies.

Finally, I would like to express my appreciation to my wife for her patience, understanding and encouragment. It is also a great pleasure to have my sons and daughters, Itqon Askary, Wafiyya Adilah, Safa Adilah, and Izzat Jundy, accompany me during my studies. I also wish to express my sincere gratitute to my parents for their moral support.

Abstract

This thesis considers the hydrodynamic solution of the linear wave interactions with a floating body at zero-speed conditions in a water body of infinite depth. The initial-boundary-value problem was linearized about the mean position of a body, and derived as a boundary integral equation for solving exterior velocity potential using Green's theorem and the impulsive Green's function in the time domain. In order to minimize time and errors in numerical evaluation, this thesis introduced the alternative solution of the time-domain free-surface Green's function based on the power series expansion method. The analytical forms in term of a power series were derived from the ordinary differential equation that were proven to be the solution of the original infinity integral of the time-domain free-surface Green's function. The purpose was to speed up the convergence of the summation of an infinite series in the numerical computation. Based on the analytical form developed, it was possible to perform procedure that speed up the evaluation of convolution integral involved in the boundary integral equation. Moreover, the singularity integral of the Rankine source was regularized and a numerical scheme using global discretization technique for regularized boundary integral equation with Gaussian quadrature was proposed. Analytical surface as well as Non-Uniform Rational B-Splines (NURBS) surfaces were employed to represent the body surface mathematically. Computed impulse response function and hydrodynamic coefficients due to radiated waves for a floating sphere and ellipsoid were compared with published results. The comparison was reasonable for all cases.

Chapter 1

Introduction

1.1 Background

In the design of a floating or submerged body, i.e ships, submarines, offshore structures etc, the ability to predict wave-induced motions and hydrodynamic loads is an essential requirement. Severe body motions can limit operability, affecting safety as well as comfort. Extreme wave-loads may lead to structural failure. Study of the wave-body interaction problem has been conducted actively over the last several decades. The domains in which numerical analysis of wave-body interaction takes place ordinarily are the frequency and time-domain. For a particular problem, one domain may be more convenient than the other and they can be related through the use of Fourier transforms.

The problem can be linearized by assuming motion to be small and time harmonic. The resulting boundary-value problem is solved using singularity distribution on the mean body boundary. The principal difficulties in the prediction of wave-body interaction in time domain analysis arise from:

- the evaluation of the time-domain free-surface Green's function,
- the computation of the convolution integral involved in the boundary integral equation,
- the singularity behaviour of the boundary integral equation, and
- the minimizing of numerical error due to discretization of the body.

1.2 Literature Review

One of the first studies on linear time-domain analysis of wave-body interactions was reported by Finkelstein (1957). This was improved through the introduction of an impulsive response approach was introduced by Cummins (1962). Adachi and Ohmatsu (1979) solved the two-dimensional problem in water of infinite depth, as well as Ikebuchi (1981) and Yeung (1982). Some numerical results of the two- and three-dimensional problems were presented by Jami and Pot (1985) who used a finite element method. Newman (1985) used time-dependent ring sources to solve impulsive response motion of an axisymmetric circular cylinder. Added mass and damping coefficients were obtained using Fourier transform of the impulsive response following Wehausen (1971).

Other works that took a linear time-domain approach include Korsmayer (1988), on the linearized radiation problem without forward speed, Ferrant (1988) for the submerged bodies case; and Liapis (1986), Beck and Liapis (1987), King (1987), King et al. (1988) on the general linearized problem with zero and constant forward speed. Results for large body motion have been obtained by Beck and Magee (1990),

who adopted the panel method to discretize the body surface and solve the problem numerically following Hess and Smith (1964). In the panel method, the body surface was discretized into finite number of panels, and each panel is defined by a plane or quadratically curved surface formula. In this way, over each panel, a collocation point is obtained, and the source density or potential distribution, which is assumed to be constant is determined.

The higher-order panel method developed by Maniar (1995) used a B-spline technique. Higher-order methods allow for linear or quadratic panels and first- or second-degree polynomial distribution of source densities or potential over a panel. A similar approach, with several modifications, has been undertaken by Lee et al (1998). Danmeier (1999) presented a geometry-independent higher-order method. Lee and Newman (2001) used a B-spline to represent the velocity potential. However, in numerical schemes those methods still produce some errors, first, because of the approximation of the surface geometry, and second, because of the assumed location of a source density distribution on each panel. The error might be reduced if the geometrical data of the body is taken from the original surface formulation, and the collocation points are adjusted on the curvature of the surface. Qiu (2001) proposed a panel-free method in order to minimize errors due to the geometrical approximation and an assumption of source strength distribution on the panel. In his work, the boundary integral equation in terms of source strength was desingularized before discretizing the body surface, following the method outlined by Landwaber and Macagno (1969). Globally, Gaussian quadrature over the exact body geometry was conducted to evaluate singularity of the integral. Non-Uniform Rational B-Splines (NURBS) surface was used to represent geometry of the body.

In the inital boundary-value problem with a linearized free-surface condition, Green's theorem is derived to solve the velocity potential of a floating or submerged

body. The original equation of the time-domain free surface Green's function, in terms of an infinity integral equation, has been given in analytic form by Wehausen and Laitone (1960). However, Ferrant (1988) noticed that the evaluation of the free-surface Green's function was excessively time-consuming; about 80 percent of the total CPU time was required to evaluate the boundary integral equation (Magee ,1991). Indeed, reduction of evaluation time of the free-surface Green's function without compromising computational accuracy is the main focus of any follow-up research.

Several previous studies have explored an alternative expression for the free-surface Green's function, based on the original integral equation. Newman (1985) has derived the technique by which the domain of free surface Green's function is divided into a number of regions wherein, depending on the arguments, ascending series, asymtotic expansion or a combination of these, and two-dimensional economized (Chebyshev) polynomial approximation were utilized. The improved version of this method has been employed by Lin and Yue (1990), and Bingham (1994). Liapis and Beck (1985) has proposed three different regions that were series expansion, asymtotic expansion, and Filon quadrature. King (1987) has followed with the additional Bessel function expansion regions on free surface Green's function evaluation.

Ferrant (1988) has proposed a new computational technique, i.e., a tabulation method, that obviously can reduce the computational time significantly. This method essentially pre-computes of the free surface Green's function on a grid of μ and τ once for all domains. The computed data was stored in several permanent files in tabulation format. A simple bilinear interpolation was used to carry out the value for each calculation. Motivated by the need to further reduce computational costs, a vectorized computational approach was introduced by Magee and Beck (1989), and it was followed by Newman (1991) and Lin and Yue (1990) who applied on a supercomputer. An innovative approach was developed by Clément (1998a). He

proved that the free surface Green's function is a solution of a fourth-order ordinary differential equation (ODE), and Runge-Kutta method could be adopted (Clément, 1998b) to evaluate the ODE Green's function numerically. Clément (1998b) has used the ODE-integration methods to evaluate the boundary integral equation of the seakeeping problem. Clément (1998b) showed that the Runge-Kutta method can be used to evaluate ODE Green's function more rapidly than the tabulation method and the series expansion method. Although the accuracy of the Runge-Kutta method for the ODE Green's function evaluation is reasonable, it does not give much advantage for the analytical form of ODE Green's function. Because of numerical errors, it can be reduced only by decreasing the time step. However, this increased the total evaluation time. There appears to be room here to propose an alternative approach closer to the analytical solution.

1.3 Objectives and Scope of the Thesis

The primary objective of this thesis is to develop an analytical form in which to evaluate the time-domain free-surface Green's function. The analytical form is derived based on ODE Green's function developed by Clément (1998a), expanded into a power series expansion. The purpose is to improve the accuracy and to reduce the length of time taken in evaluation of the time-domain free-surface Green's function.

Secondly, based on the analytical form of the free-surface Green's function, a numerical procedure to carry out the convolution integral involved in the boundary integral equation is performed. The accuracy and efficiency of the approach developed are demonstrated by comparison against the Runge-Kutta method and a tabulation method.

Thirdly, the singularity of the boundary integral equation is regularized based on Landwaber and Macagno's approach (1969) for solving the exterior velocity potential problem. An analytical surface, as well as Non-Uniform Rational B-Splines (NURBS) surface, are developed to represent the geometry of the body surface mathematically, in which the Gaussian points can be generated over the body surface globally. Following this, a numerical scheme for regularized boundary integral equation with Gaussian Quadrature is imposed.

Fourthly, floating bodies -spherical and ellipsoidal- are evaluated respectively. The results of the new approach are compared against the available analytical solution, as well as other numerical methods. The superiority of the new approach is illustrated in terms of root mean square (RMS) error and elapsed time (ET) for several cases.

1.4 Overview of the thesis

This thesis is divided into six chapters. After the introductory chapter (Chapter 1), Chapter 2 gives the mathematical formulation of the linear initial-boundary-value problem for the wave-body interaction. In the linear problem, the body boundary condition and the free-surface condition are linearized in which the time-domain Green's function approach is used to satisfy both conditions. The boundary integral equation is derived using Green's identity and the impulsive theorem in order to find the velocity potential. The regularized method is applied to remove the singularity involved in the boundary integral. The transient free-surface Green's function which is involved in the boundary integral is evaluated in Chapter 3 analytically. In Chapter 4, the numerical solution of the boundary integral equation is performed using the one-panel method. Numerical results for the case of motion of a floating sphere and

ellipsoid are presented in Chapter 5. Conclusions are given in Chapter 6.

Chapter 2

Theoretical Formulation

2.1 Co-ordinate System

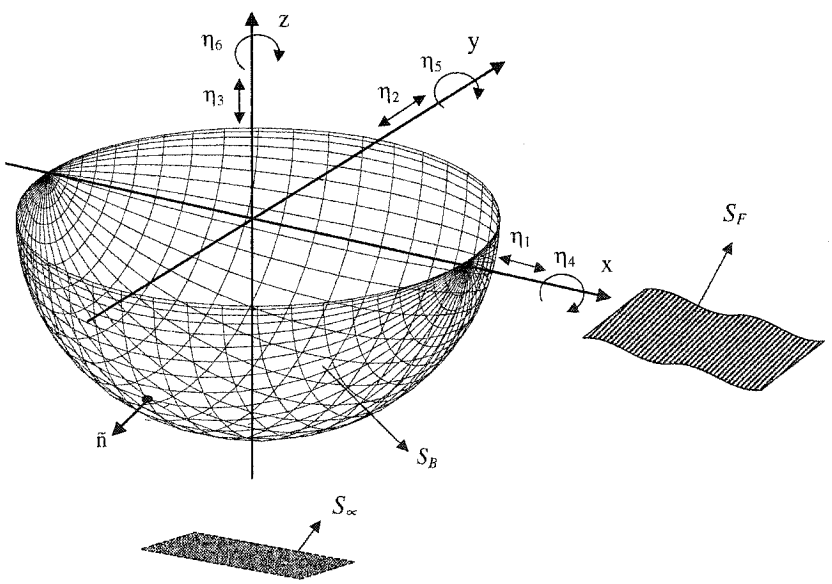

Figure 2.1: The co-ordinate system definition

The co-ordinate system shown in Figure 2.1 illustrates the problem under consideration. The Cartesian co-ordinate system $0xyz$ is fixed to the mean position of the body in space. The z-axis is vertically upwards and through the center of gravity of the body. The x and y lie in the undisturbed plane of the free surface and the origin is at the midship at $z = 0$, in a semi-infinite fluid, S_∞. The fluid domain is denoted by Ω, the free surface by S_F, and the body surface by S_B.

The rigid-body motion is described by the six-component vector $\vec{\eta}_k$ of displacements and rotations from initial position. The six components of the motion of the body are: η_1 = surge, η_2 = sway, and η_3 = heave due to translation, η_4 = roll, η_5 = pitch, and η_6 = yaw due to rotation.

2.2 Initial Boundary Value Problem

The problem here deals with a floating body on the free-surface in a semi-infinite fluid without forward speed. The amplitude of motion is assumed small, and the linearized time-domain analysis applicable. The fluid is assumed incompressible, inviscid, and irrotational, and the fluid velocity in terms of the velocity potential, $\phi(x, y, z; t)$ can be written as

$$\vec{U} = \nabla\phi(x, y, z; t) \tag{2.1}$$

The governing equation of motion is given by the Laplace equation:

$$\nabla^2\phi(x, y, z; t) = 0 \tag{2.2}$$

Analyzing the linear body motion without speed, the unsteady oscillation body is considered. The potential, $\phi(x, y, z; t)$ due to unsteady motion is then defined by separating into two distinctive parts, such as:

$$\phi(x, y, z; t) = \phi_R(x, y, z; t) + \phi_D(x, y, z; t) \tag{2.3}$$

where,

$$\begin{aligned} \phi_R(x, y, z; t) &= \sum_{k=1}^{6} \phi_k(x, y, z, t) \qquad (2.4) \\ \phi_1, ..., \phi_6 &= \text{the velocity potential due to radiated wave} \\ &\quad \text{(surge, sway, heave, roll, pitch, and yaw respectively)} \\ \phi_D &= \text{the velocity potensial due to diffracted wave} \end{aligned}$$

The diffraction potential consists of an incident wave potential,ϕ_I, and the scattering wave potential, ϕ_7, yielding

$$\phi_D(x, y, z; t) = \phi_I(x, y, z; t) + \phi_7(x, y, z; t) \tag{2.5}$$

Since the amplitude of the wave elevation is assumed small compared to its characteristic wave length, the free-surface condition can be linearized. On the free-surface, the dynamic boundary condition is

$$\frac{\partial \phi(x,y,z;t)}{\partial t} + g\varsigma = 0 \qquad \text{on z} = 0 \tag{2.6}$$

and kinematic boundary condition is

$$\frac{\partial \phi(x,y,z;t)}{\partial z} - \frac{\partial \varsigma}{\partial t} = 0 \qquad \text{on z} = 0 \tag{2.7}$$

where ς is the free-surface elevation. Combining the Eqn (2.6) and Eqn (2.7), the linearized free-surface boundary condition may be expressed by the single equation,

$$\frac{\partial^2 \phi(x,y,z;t)}{\partial t^2} + g\frac{\partial \phi(x,y,z;t)}{\partial z} = 0 \qquad z = 0 \tag{2.8}$$

where g is the acceleration due to gravity. Without the fluid viscosity, the no-flux condition must be imposed on the body boundary, which is defined that the normal velocity of the fluid must be equal to the normal velocity of the body boundary enforced on the exact position of the body surface, $S_B(t)$:

$$\frac{\partial \phi_k(x,y,z;t)}{\partial n} = \dot{\eta}.\vec{n}_k \qquad \text{for} \quad k = 1,2,...,6 \tag{2.9}$$

$$\frac{\partial \phi_7(x,y,z;t)}{\partial n} = -\frac{\partial \phi_I}{\partial n} \tag{2.10}$$

where $\dot{\eta}$ is an instantaneous velocity of a point on the body surface, and n_k is an outward unit normal to the fluid, out of the body surface defined as

$$\begin{aligned} \vec{n}_k &= \{n_1, n_2, n_3\} \\ \vec{r} \times \vec{n}_k &= \{n_4, n_5, n_6\} \\ \vec{r} &= (x, y, z) \end{aligned} \tag{2.11}$$

The fluid velocities on free surface caused by the body must go to zero such as,

$$\nabla\phi(x, y, z; t) \to 0 \qquad R = \sqrt{x^2 + y^2} \to \infty \qquad \text{on } z = 0 \tag{2.12}$$

and the boundary condition on the bottom is obtained as

$$\frac{\partial\phi(x, y, z; t)}{\partial z} = 0 \qquad z \to -\infty \tag{2.13}$$

Two initial conditions are required, since the free-surface condition is second order in time.

$$\phi(x, y, z; t) = 0, \qquad \frac{\partial\phi(x, y, z; t)}{\partial t} = 0 \qquad \text{on } \; z = 0, \qquad t \leq t_0 \tag{2.14}$$

where t_0 is some arbitrary starting time for the fluid motions it will be taken to be zero in the radiation problem and $-\infty$ in the scattering problem.

2.3 The Boundary Integral Equation

The hydrodynamic or radiation forces on the body surface are investigated, and only the potential ϕ_k with $k = 1, 2...6$ on the body surface is needed. The values of ϕ_k on the free surface and at infinity vanish [see Appendix A]. The body surface can be represented as distribution source velocity potential. The source potential is also known as the transient Green's function denoted as G. We define $P(x_P, y_P, z_P)$ as a field point and $Q(x_Q, y_Q, z_Q)$ as a source point, in the $0xyz$ co-ordinate system. The transient Green's function, G, is given in analytic form by Wehausen and Laitone (1960) and it was split into two terms. The first term represents the potential at the field point P at time t due to an impulsive source at the point Q at time τ. The second term represents the wave system that are generated by impulsive source in underwater disturbance. The expression of G is:

$$G(P, Q; t-\tau) = \delta(t-\tau)G_0(P, Q) + H(t-\tau)\tilde{F}(P, Q; t-\tau) \tag{2.15}$$

where $\delta(t-\tau)$ is the Dirac delta function; $H(t-\tau)$ is the Heaviside unit step function; the Rankine source is,

$$G_0(P, Q) = \frac{1}{r_{PQ}} - \frac{1}{r_{P\bar{Q}}} \tag{2.16}$$

and the memory effect is

$$\tilde{F}(P,Q;t-\tau) = 2\int_0^\infty J_0(kR)e^{k\zeta}\sqrt{kg}\sin[\sqrt{kg}(t-\tau)]dk \tag{2.17}$$

with $R = \sqrt{(x_P - x_Q)^2 + (y_P - y_Q)^2)}$; $\zeta = z_P + z_Q$; $r_{PQ} = \sqrt{R^2 + (z_P - z_Q)^2}$; and $r_{P\bar{Q}} = \sqrt{R^2 + \zeta^2}$. J_0 is the Bessel function of the *zero*th order.

Since the Green's function as potential source moving under a free surface, the Green's function solves the following boundary value problem of the free surface hydrodynamic, which are a Poisson's equation

$$\nabla_Q^2 G(P,Q;t-\tau) = -4\pi\delta(P-Q)\delta(t-\tau), \qquad \text{for } t \geq 0,\ z_Q < 0 \tag{2.18}$$

Initial condition

$$G(P,Q;0) = 0, \qquad \frac{\partial G}{\partial \tau}(P,Q;0) = 0, \qquad \text{for } z_Q \leq 0 \tag{2.19}$$

Boundary condition

$$\frac{\partial^2 G}{\partial \tau^2}(P,Q;t-\tau) + g\frac{\partial G}{\partial z_Q}(P,Q;t-\tau) = 0, \qquad \text{for } t \geq 0, z_Q = 0 \tag{2.20}$$

Infinite condition

$$\lim_{r\to\infty} |\nabla_Q G(P,Q;t-\tau)| = 0, \tag{2.21}$$

The boundary integral equation for solving the velocity potential is derived by applying the Green's second identity, in the fluid domain Ω.

$$\int_{V_Q} \left\{ \phi_k(Q,\tau) \nabla_Q^2 G(P,Q;t-\tau) - G(P,Q;t-\tau) \nabla_Q^2 \phi_k(Q,\tau) \right\} dV_Q$$
$$= \int_{S_Q} \left\{ \phi_k(Q,\tau) \frac{\partial G}{\partial n_Q}(P,Q;t-\tau) - G(P,Q;t-\tau) \frac{\partial \phi_k}{\partial n_Q}(Q,\tau) \right\} dS_Q \quad (2.22)$$

where the volume V_Q is bounded by S_Q, and $S_Q = S_B + S_F + S_\infty$. S_B, S_F and S_∞ are body surface, free surface and bounding surface at infinity, respectively. Left hand side of Eqn (2.22) can be simplified satisfying for Poisson's equation (2.18) and Laplace's equation (2.2); and using equivalent of the impulsive formula [see Rahman (1991)] yields:

$$\begin{aligned} -4\pi\phi_k(P,\tau)\delta(t-\tau) &= \int_{S_Q(\tau)} \left\{ \phi_k(Q,\tau) \frac{\partial G}{\partial n_Q}(P,Q;t-\tau) \right. \\ &- \left. \frac{\partial \phi_k}{\partial n_Q}(Q,\tau) G(P,Q;t-\tau) \right\} dS_Q, \qquad P \in \Omega \end{aligned} \quad (2.23)$$

Considering the field point on the body surface, S_B, Eqn (2.23) is integrated both left and right hand sides of Eqn (2.23) with respect to τ from 0 to t, and then using the impulsive formula [see Rahman (1991)] yields,

$$\begin{aligned} -2\pi\phi_k(P,t) &= \int_0^t d\tau \int_{S_B(\tau)} \left\{ \phi_k(Q,\tau) \frac{\partial G}{\partial n_Q}(P,Q;t-\tau) \right. \\ &- \left. \frac{\partial \phi_k}{\partial n_Q}(Q,\tau) G(P,Q;t-\tau) \right\} dS_Q, \qquad P \in S_B \end{aligned} \quad (2.24)$$

We obtained the integral representation of the velocity potential in the fluid domain Ω, in terms of a mixed distribution of sources and normal dipoles on S_B. Now substituting Eqn (2.15) into Eqn (2.24), and satisfy the Dirac delta function and the Heaviside step function. Therefore, the boundary integral equation to evaluate the velocity potential, ϕ_k is obtained as

$$\begin{aligned} 2\pi\phi_k(P,t) \;+\; & \int_{S_B(t)} \phi_k(Q,t)\frac{\partial}{\partial n_Q}\Big(\frac{1}{r_{PQ}} - \frac{1}{r_{P\bar{Q}}}\Big)dS_Q \\ = \; & \int_{S_B(t)} \frac{\partial \phi_k}{\partial n_Q}(Q,t)\Big(\frac{1}{r_{PQ}} - \frac{1}{r_{P\bar{Q}}}\Big)dS_Q \\ - \; & \int_0^t d\tau \int_{S_B(\tau)} \Big\{\phi_k(Q,\tau)\frac{\partial \tilde{F}}{\partial n_Q}(P,Q;t-\tau) \\ - \; & \tilde{F}(P,Q;t-\tau)\frac{\partial \phi_k}{\partial n_Q}(Q,\tau)\Big\}dS_Q \qquad P \in S_B \end{aligned} \tag{2.25}$$

Eqn (2.25) is in the typical form of a Fredholm-Volterra integral equation for the unknown potential on the body surface. The Fredholm kernel which is a Rankine source or singular part of Green's function is independent of time, and it can be evaluated for one time at $t = 0$ for all time evaluations. The Volterra kernel is time dependent so that the evaluation of the kernel which is the memory part of Green's function is performed for each time step for $t > 0$. However, the difficult part of Eqn (2.25) evaluation is to solve the singularity of integral and the memory effect of Green's function $\tilde{F}$ involved in the convolution integral. The singularity integral will be evaluated by using the regularized approach in the next section. The analytical procedure to evaluate the memory effect of Green's function will be demonstrated in detail in Chapter 3.

2.4 Regularized Boundary Integral Equation

It is shown in Eqn (2.25) that the free-surface effects, $\tilde{F}(P;t,Q;\tau)$ are absent in the limit $t=0$. The integral equation involves only the singular part or the Rankine ring source and its negative image above the free surface. The general Regularized method solution for the potential flow problem which is based on Landweber and Macagno (1969) will be extended. Therefore, when $t=0$, Eqn (2.25) can be rewritten as:

$$\begin{aligned} 2\pi\phi_k(P,0) \;+\; & \int_{S_B(t)} \phi_k(Q,0)\frac{\partial}{\partial n_Q}\Big(\frac{1}{r_{PQ}}-\frac{1}{r_{P\bar{Q}}}\Big)dS_Q \\ = \; & \int_{S_B(t)} q_k(Q)\Big(\frac{1}{r_{PQ}}-\frac{1}{r_{P\bar{Q}}}\Big)dS_Q \end{aligned} \tag{2.26}$$

where $q_k(Q)=\frac{\partial\phi_k}{\partial n_Q}(Q,0)$, and by adding and subtracting of Eqn (2.26), yields,

$$\begin{aligned} 2\pi\phi_k(P;0) \;=\; & \int_{S_B}\Big\{\phi_k(Q;0)\nabla_Q\Big[\frac{1}{r_{PQ}}+\frac{1}{r_{P\bar{Q}}}\Big].\vec{n}_Q - q_k(Q)\Big[\frac{1}{r_{PQ}}+\frac{1}{r_{P\bar{Q}}}\Big]\Big\}dS_Q \\ & -2\int_{S_B}\Big\{\phi_k(Q;0)\nabla_Q\Big[\frac{1}{r_{P\bar{Q}}}\Big].\vec{n}_Q - q_k(Q)\Big[\frac{1}{r_{P\bar{Q}}}\Big]\Big\}dS_Q \end{aligned} \tag{2.27}$$

Introducing the Gauss flux theorem states that the flux through a closed surface due to a unit source on the same surface is 2π such as [See Jaswon and Symm (1977) for details],

$$\int_{S_B}\nabla_Q\Big[\frac{1}{r_{PQ}}+\frac{1}{r_{P\bar{Q}}}\Big].\vec{n}_Q dS_Q = -2\pi \tag{2.28}$$

and substituting it into Eqn (2.27) yield,

$$4\pi\phi_k(P;0) = \int_{S_B}\Big\{\Big[\phi_k(Q;0)-\phi_k(P;0)\Big]\nabla_Q\Big[\frac{1}{r_{PQ}}+\frac{1}{r_{P\bar{Q}}}\Big].\vec{n}_Q - q_k(Q)\Big[\frac{1}{r_{PQ}}+\frac{1}{r_{P\bar{Q}}}\Big] -2\int_{S_B}\Big\{\phi_k(Q;0)\frac{\partial}{\partial n_Q}\Big[\frac{1}{r_{P\bar{Q}}}\Big]-q_k(Q)\Big[\frac{1}{r_{P\bar{Q}}}\Big]\Big\}dS_Q \tag{2.29}$$

By adding and substracting of Eqn (2.29) with the following term,

$$\int_{S_B} q_k(P)\frac{\delta(Q)}{\delta(P)}\Big[\frac{1}{r_{PQ}}+\frac{1}{r_{P\bar{Q}}}\Big]\Big\}dS_Q \tag{2.30}$$

and introducing the potential constant ϕ_e given as,

$$\phi_e = -\int_{S_B}\delta(Q)\Big[\frac{1}{r_Q}+\frac{1}{r_{\bar{Q}}}\Big]dS_Q \tag{2.31}$$

where $\delta(Q)$ is the potential distributed on S_B which makes the body surface an equipotential surface of potential ϕ_e and satisfying the following integral,

$$\int_{S_B}\Big\{\delta(Q)\nabla_P\Big[\frac{1}{r_{PQ}}+\frac{1}{r_{P\bar{Q}}}\Big].\vec{n}_P - \delta(P)\nabla_Q\Big[\frac{1}{r_{PQ}}+\frac{1}{r_{P\bar{Q}}}\Big].\vec{n}_Q\Big\}dS_Q = 0 \tag{2.32}$$

Therefore, Eqn (2.29) can be summarized as

$$
\begin{aligned}
4\pi\phi_k(P;0) &= \int_{S_B}\Big\{\Big[\phi_k(Q;0)-\phi_k(P;0)\Big]\nabla_Q\Big[\frac{1}{r_{PQ}}+\frac{1}{r_{P\bar{Q}}}\Big].\vec{n}_Q \\
&- \Big[q_k(Q)-q_k(P)\frac{\delta(Q)}{\delta(P)}\Big]\Big[\frac{1}{r_{PQ}}+\frac{1}{r_{P\bar{Q}}}\Big]\Big\}dS_Q+\frac{\phi_e}{\delta(P)}q_k(P) \\
&- 2\int_{S_B}\Big\{\phi_k(Q;0)\nabla_Q\Big[\frac{1}{r_{P\bar{Q}}}\Big].\vec{n}_Q-q_k(Q)\Big[\frac{1}{r_{P\bar{Q}}}\Big]\Big\}dS_Q \qquad (2.33)
\end{aligned}
$$

An iterative formula for finding δ of Eqn (2.32) may be written as,

$$
\begin{aligned}
\delta^{(k+1)}(P) &= \delta^{(k)}(P)+\frac{1}{2\pi}\int_{S_B}\Big\{\delta^{(k)}(Q)\nabla_P\Big[\frac{1}{r_{PQ}}+\frac{1}{r_{P\bar{Q}}}\Big].\vec{n}_P \\
&- \delta^{(k)}(P)\nabla_Q\Big[\frac{1}{r_{PQ}}+\frac{1}{r_{P\bar{Q}}}\Big].\vec{n}_Q\Big\}dS_Q \qquad (2.34)
\end{aligned}
$$

The discretizing of Eqn (2.33) and (2.34) with Gaussian quadrature will be performed in Chapter 4.

2.5 The Hydrodynamic Force

The hydrodynamic or radiation forces acting on the body due to the fluid disturbance caused by body motion are found by integrating the pressure over the body surface. The generalized force on the body in jth direction is given as:

$$
F_j^R(t)=\int_{S_B}p(P,t)n_j dS_P \qquad j=1,2,3 \qquad (2.35)
$$

where n_j, representing the generalized unit normal as defined in Eqn (2.11), $j = 1, 2, 3$ coresponds to the directions of the x, y, z axes respectively, and $p(P, t)$ is the hydrodynamic pressure is given by Bernoulli's equation.

$$p(P,t) = -\rho(\phi_t + \frac{1}{2}|\nabla|^2 + gz_0) + p_a \tag{2.36}$$

where ϕ_t denotes the partial differentiation on ϕ with respect to time t, ρ is the fluid density, g is the acceleration of gravity, and z_0 is the z-coordinate of a point on the free surface. Since the oscillatory motion of the body and fluid are assumed to be small, the second-order terms of Bernoulli's equation can be neglected, resulting in the following equation,

$$p(P,t) = -\rho\frac{\partial\phi_k}{\partial t}(P,t) \tag{2.37}$$

where ϕ_k is the potential which describes the fluid disturbance caused by kth mode motion. The hydrodynamic force on the body in the jth direction due to arbitrary motion in mode kth can be defined by substituting Eqn (2.37) into (2.35) in the following form:

$$F_{jk}^R(t) = -\rho\int_{S_B}\frac{\partial\phi_k}{\partial t}(P,t)n_j dS_P \qquad k = 1, 2, ..., 6 \tag{2.38}$$

2.5.1 Impulse Response Function

In this section, the hydrodynamic force as a result of the impulsive motion is formulated. The body is defined as linear system in which the ship motion in each kth mode represents an input and the hydrodynamic force is an output of the system. In this case, the impulse response function represents the characterization of the body linear system. The theory of impulsive-response function for linearized ship motions as introduced by Cummins (1962) and elaborated by Ogilvie (1964), is followed. Ogilvie (1964) proposed an instantaneous velocity of the body surface $\dot{\eta}$ is equal to $\delta(t)$ and decompose the velocity potential ϕ_k as,

$$\phi_k(P,t) = \phi_k^{(0)}(P,0)\delta(t) + \phi_k^{(t)}(P,t) \tag{2.39}$$

where the first part on the right-hand side (RHS) of Eqn (2.39) represents the impulsive part of body motion, which is the condition at $t = 0$, and the second part is the time history of the fluid disturbance caused by the initial impulse of the first part which is the condition at $t > 0$. Liapis (1986) show the potential for an arbitrary forced motion in the k^{th} direction is defined as the convolution of $\phi_k(P,t)$ with the velocity of the motion, and it is expressed as,

$$\phi_k(P,t) = \int_0^t \phi_k(P,t-\tau)\dot{\eta}_k(\tau)d\tau \tag{2.40}$$

Eqn (2.40) can be also decomposed into two terms such as,

$$\phi_k^{(0)}(P,0) = \int_0^t \phi_k^{(0)}(P,0)\dot{\eta}_k(\tau)d\tau \tag{2.41}$$

$$\phi_k^{(t)}(P,t) = \int_0^t \phi_k^{(t)}(P,t-\tau)\dot{\eta}_k(\tau)d\tau \tag{2.42}$$

Substituting both Eqn (2.41) and (2.42) into the right hand side of Eqn (2.39) and considering the integration of delta function yield:

$$\phi_k(P,t) = \phi_k^{(0)}(P,0)\dot{\eta}_k(t) + \int_0^t \phi_k^{(t)}(P,t-\tau)\dot{\eta}_k(\tau)d\tau \tag{2.43}$$

The hydrodynamic force acting to the body, F_{jk}^R is given, by substituting Eqn (2.43) into Eqn (2.38) and considering the Leibnitz-rule of differentiation under integral sign [see Wylie and Barret (1982) for details], yielding:

$$\begin{aligned} -F_{jk}^R(t) &= \rho\ddot{\eta}_k(t)\int_{S_B}\phi_k^{(0)}(P,0)n_j dS_P + \rho\dot{\eta}_k(t)\int_{S_B}\phi_k^{(t)}(P,0)n_j dS_P \\ &+ \rho\int_0^t\int_{S_B}\frac{\partial\phi_k^{(t)}}{\partial t}(P,t-\tau)\dot{\eta}_k(\tau)n_j dS_P d\tau \end{aligned} \tag{2.44}$$

and Eqn (2.44) can be simplified as:

$$-F_{jk}^R(t) = \mu_k\ddot{\eta}_k(t) + \lambda_k\dot{\eta}_k(t) + \int_0^t K_{jk}^R(t-\tau)\dot{\eta}_k(\tau)d\tau \tag{2.45}$$

with

$$\mu_{jk} = \rho \int_{S_B} \phi_k^{(0)}(P,0) n_j dS_P \tag{2.46}$$

$$\lambda_{jk} = \rho \int_{S_B} \phi_k^{(t)}(P,0) n_j dS_P \tag{2.47}$$

$$K_{jk}^R(t-\tau) = \rho \int_{S_B} \frac{\partial \phi_k^{(t)}}{\partial t}(P,t-\tau) n_j dS_P \tag{2.48}$$

where μ_{jk} is the infinite fluid added mass, and is a function of the body geometry. The term, λ_{jk} is the damping coefficient, and it is a function of the body geometry. $K_{jk}^R(t)$ is an impulse response function for a linear system, and depends on time and geometry of body, but it is independent of the past time history of the motion.

2.5.2 Added Mass and Damping

The motion of a floating body can be considered to be a harmonic function of time with a frequency, ω. The hydrodynamic force acting on a floating body for sinusoidal motion in frequency domain is given as,

$$-F_{jk}^R(\omega) = e^{i\omega t}(-\omega^2 A_{jk}(\omega) + i\omega B_{jk}(\omega) + C_{jk}) \tag{2.49}$$

Substituting $\eta(t) = e^{i\omega t}$ into (2.45), and neglecting the hydrostatic restoring force, C_{jk}, in Eqn (2.49), the time-dependent impulsive response function can be related to the frequency-dependent coefficient as follows:

$$e^{i\omega t}\Big(-\omega^2 A_{jk}(\omega)+i\omega B_{jk}(\omega)\Big)=e^{i\omega t}\Big(-\omega^2\mu_{jk}+i\omega\lambda_{jk}+i\omega\int_0^t K_{jk}^R(\tau)e^{-i\omega\tau}d\tau\Big) \quad (2.50)$$

Equating real and imaginary parts of Eqn (2.50) yields,

$$A_{jk}(\omega) = \mu_{jk}-\frac{1}{\omega}\int_0^t K_{jk}^R(\tau)\sin\omega\tau d\tau \quad (2.51)$$

$$B_{jk}(\omega) = \lambda_{jk}+\int_0^t K_{jk}^R(\tau)\cos\omega\tau d\tau \quad (2.52)$$

where $A_{jk}(\omega)$ and $B_{jk}(\omega)$ are the added-mass and damping coefficients of the linear frequency domain respectively.

Chapter 3

The Transient Free-surface Green's Function and Analytical Solutions

In evaluating the boundary integral equation (Eqn 2.25), for t greater than 0, the free surface effect, $\tilde{F}(P,Q;t)$, is considered. It is shown that the major part of the total computing time required for the numerical computation of Eqn (2.25) is spent to evaluate the $\tilde{F}(P,Q;t)$ function because of the convolution integral. The $\tilde{F}(P,Q;t)$ function has to be evaluated for each location of the field, P, and source, Q, at every time step. Several approaches have been developed in order to reduce the time consumed and the numerical error of $\tilde{F}(P,Q;t)$ function evaluation. These were reviewed in Chapter 1.

In this chapter, the $\tilde{F}(P,Q;t)$ function is formulated in terms of the natural variables $\tilde{F}(\mu,\beta)$. Therefore, an analytical approach is developed to evaluate the $\tilde{F}(\mu,\beta,)$ function, based on Clément's approach (1998a). Since the new approach is developed for the domain $\mu \geq 0$, the analytical expression for $\mu = 0$ and $\mu = 1$ are explored as well to verify the new approach, respectively. Some numerical computations of the

$\tilde{F}(\mu, \beta,)$ function evaluation are presented. The numerical performance of the new approach is demonstrated in comparison to the established method,i.e., tabulation method and Runge-Kutta method, in certain cases. The implementation of the new approach into the convolution integral equation solution is performed.

3.1 The Free-surface Green's Function

As was mention in the previous chapter, the solution of the initial boundary value problem with a linearized free-surface condition for the velocity potential to a floating body is derived from the Green's theorem. The fundamental solution of this case is addressed to the source potential which satisfies the free-surface condition, i.e. the free-surface Green's function. The principal free-surface Green's function has been given by Wehausen and Laitone (1960) as,

$$\tilde{F}(P, Q; t) = 2 \int_0^\infty J_0(kR) e^{k\zeta} \sqrt{kg} \sin[\sqrt{kg}t] dk \tag{3.1}$$

where $P(x_P, y_P, z_P)$ is a field point and $Q(x_Q, y_Q, z_Q)$ is a source point, in the $0xyz$ co-ordinate system, $R = \sqrt{(x_P - x_Q)^2 + (y_P - y_Q)^2}$, $\zeta = z_P + z_Q$, $r_{PQ} = \sqrt{R^2 + (z_P - z_Q)^2}$, $r_{P\bar{Q}} = \sqrt{R^2 + \zeta^2}$, and J_0 is the Bessel function of the $zero$th order. Typical of Eqn (3.1) is the infinity integral, and it is interpreted as transforms in wavenumber space over the free surface domain. The time dependence is harmonic with a prescribed frequency, ω. Since the integrands are highly oscillatory, direct numerical integration is inefficient, especially when the field point, P, and the source point, Q, are close to the free surface. It is more convinient for analytical evaluation to non-dimensionalize

the physical parameters with respect to g and $r_{P\bar{Q}}$. The variable t is replaced by β, and let write the new variables,

$$\lambda = kr_{P\bar{Q}}; \qquad \mu = -\frac{\zeta}{r_{P\bar{Q}}}; \qquad \beta = t\sqrt{\frac{g}{r_{P\bar{Q}}}}$$

Then,

$$kR = \lambda\sqrt{(1-\mu^2)}; \qquad \sqrt{kg} = \sqrt{\frac{g\lambda}{r_{P\bar{Q}}}}$$

$$k\zeta = -\lambda\mu; \qquad dk = \frac{1}{r_{P\bar{Q}}}d\lambda$$

Therefore, Eqn (3.1) can be re-written as

$$\tilde{F}(P,Q;t) = 2\sqrt{\frac{g}{r_{P\bar{Q}}^3}}F_1(\mu,\beta) \tag{3.2}$$

where

$$F_1(\mu,\beta) = \int_0^\infty J_0(\sqrt{(1-\mu^2)}\lambda)e^{-\lambda\mu}\sqrt{\lambda}\sin(\beta\sqrt{\lambda})d\lambda \tag{3.3}$$

The parameter μ relates the depth of submergence to the horizontal distance, R, with the range value $0 \leq \mu \leq 1$. The parameter, β, is related to the phase of the generated

waves.

Also, in the evaluation of boundary integral equation (Eqn 2.25), the normal of $\tilde{F}(P,Q;t)$ function has to be defined yielding

$$\frac{\partial \tilde{F}}{\partial n_Q}(P,Q;t) = \vec{n}_{x_Q}\frac{\partial \tilde{F}}{\partial x_Q}(P,Q;t) + \vec{n}_{y_Q}\frac{\partial \tilde{F}}{\partial y_Q}(P,Q;t) + \vec{n}_{z_Q}\frac{\partial \tilde{F}}{\partial Z_Q}(P,Q;t) \tag{3.4}$$

By rendering various terms non-dimensional, one obtains

$$\frac{\partial \tilde{F}}{\partial x_Q}(P,Q;t) = -2\sqrt{\frac{g}{r^3_{P\bar{Q}}}}\frac{x_Q - x_P}{r_{P\bar{Q}}R}F_2(\mu,\beta) \tag{3.5}$$

$$\frac{\partial \tilde{F}}{\partial y_Q}(P,Q;t) = -2\sqrt{\frac{g}{r^3_{P\bar{Q}}}}\frac{y_Q - y_P}{r_{P\bar{Q}}R}F_2(\mu,\beta) \tag{3.6}$$

$$\frac{\partial \tilde{F}}{\partial z_Q}(P,Q;t) = 2\sqrt{\frac{g}{r^3_{P\bar{Q}}}}\frac{1}{r_{P\bar{Q}}R}F_3(\mu,\beta) \tag{3.7}$$

where

$$F_2(\mu,\beta) = \int_0^\infty J_1(\sqrt{(1-\mu^2)}\lambda)e^{-\lambda\mu}\lambda\sqrt{\lambda}\sin(\beta\sqrt{\lambda})d\lambda \tag{3.8}$$

$$F_3(\mu,\beta) = \int_0^\infty J_0(\sqrt{(1-\mu^2)}\lambda)e^{-\lambda\mu}\lambda\sqrt{\lambda}\sin(\beta\sqrt{\lambda})d\lambda \tag{3.9}$$

3.2 Analytical Solution of F_1, F_2, and F_3

The solution of Eqn (3.3), Eqn (3.8), and Eqn (3.9) can be expressed into nine terms of fourth order ordinary differential equation. The procedure of derivation is based on Clément's approach (1998a) and it is described in Appendix B. The nine terms of fourth order ordinary differential equation as the solution of Eqn (3.3) is

$$\begin{aligned} &x_1\frac{d^4F_1}{d\beta^4} + x_2(\beta-\beta_1)\frac{d^3F_1}{d\beta^3} + x_3\frac{d^3F_1}{d\beta^3} + x_4(\beta-\beta_1)^2\frac{d^2F_1}{d\beta^2} \\ &+x_5(\beta-\beta_1)\frac{d^2F_1}{d\beta^2} + x_6\frac{d^2F_1}{d\beta^2} + x_7(\beta-\beta_1)\frac{dF_1}{d\beta}(\beta) \\ &+x_8\frac{dF_1}{d\beta} + x_9F_1 = 0 \end{aligned} \tag{3.10}$$

where

$$\begin{aligned} &x_1 = 1;\ x_2 = \mu;\ x_3 = \mu\beta_1;\ x_4 = \frac{1}{4};\ x_5 = \frac{1}{2}\beta_1; \\ &x_6 = \frac{1}{4}\beta_1^2 + 4\mu;\ x_7 = \frac{7}{4};\ x_8 = \frac{7}{4}\beta_1;\ x_9 = \frac{9}{4} \end{aligned} \tag{3.11}$$

and subject to the initial conditions,

$$\begin{aligned} F_1(\mu,0) &= 0; \qquad \frac{dF_1}{d\beta}(\mu,0) = \mu; \\ \frac{d^2F_1}{d\beta^2}(\mu,0) &= 0; \qquad \frac{d^3F_1}{d\beta^3}(\mu,0) = -3\mu + 1 \end{aligned} \tag{3.12}$$

The solution of $F_2(\mu,\beta)$ and $F_3(\mu,\beta)$ functions in Eqn (3.8) and Eqn (3.9) repectively can also be expanded into nine terms similar to Eqn (3.10). The nine variable coefficients of $F_2(\mu,\beta)$ are described as

$$\begin{aligned} &y_1 = 1;\ y_2 = \mu;\ y_3 = \mu\beta_1;\ y_4 = \frac{1}{4};\ y_5 = \frac{1}{2}\beta_1; \\ &y_6 = \frac{1}{4}\beta_1^2 + 4\mu;\ y_7 = \frac{11}{4};\ y_8 = \frac{11}{4}\beta_1;\ y_9 = \frac{21}{4} \end{aligned} \tag{3.13}$$

subject to the intial conditions,

$$\begin{aligned} F_2(\mu,0) &= 0; \qquad \frac{dF_2}{d\beta}(\mu,0) = 3\mu\sqrt{1-\mu^2}; \\ \frac{d^2F_2}{d\beta^2}(\mu,0) &= 0; \qquad \frac{d^3F_2}{d\beta^3}(\mu,0) = (3-15\mu^2)\sqrt{1-\mu^2} \end{aligned} \tag{3.14}$$

and the nine variable coefficients of $F_3(\mu,\beta)$ functions can be defined as:

$$z_1 = 1;\ z_2 = \mu;\ z_3 = \mu\beta_1;\ z_4 = \frac{1}{4};\ z_5 = \frac{1}{2}\beta_1;$$

$$z_6 = \frac{1}{4}\beta_1^2 + 4\mu;\ z_7 = \frac{11}{4};\ z_8 = \frac{11}{4}\beta_1;\ z_9 = \frac{25}{4} \tag{3.15}$$

subject to the initial conditions

$$\begin{aligned} F_3(\mu,0) &= 0; \qquad \frac{dF_3}{d\beta}(\mu,0) = 1 - 3\mu^2; \\ \frac{d^2F_3}{d\beta^2}(\mu,0) &= 0; \qquad \frac{d^3F_3}{d\beta^3}(\mu,0) = 15\mu^3 - 9\mu \end{aligned} \tag{3.16}$$

3.2.1 The Power Series Expansion

Due to the fact that the $F_1(\mu,\beta)$ function shown in Eqn (3.10) is linear with variable coefficients, the solution can be expanded in power series with respect to $\beta = \beta_1$, where β_1 is a constant. The solution of Eqn (3.10) can be expressed in terms of a power series as.

$$F_1(\beta) = a_0 + \sum_{m=1}^{\infty} a_m(\beta - \beta_1)^m \tag{3.17}$$

Eqn (3.17) is expressed in first, second, third and fourth derivations, yielding

$$F_1^{'}(\beta) = a_1 + \sum_{m=2}^{\infty} m a_m(\beta - \beta_1)^{m-1}$$

$$
\begin{aligned}
F_1''(\beta) &= 2a_2 + \sum_{m=3}^{\infty} m(m-1)a_m(\beta-\beta_1)^{m-2} \\
F_1'''(\beta) &= 6a_3 + \sum_{m=4}^{\infty} m(m-1)(m-2)a_m(\beta-\beta_1)^{m-3} \\
F_1''''(\beta) &= 24a_4 + \sum_{m=5}^{\infty} m(m-1)(m-2)(m-3)a_m(\beta-\beta_1)^{m-4} \qquad (3.18)
\end{aligned}
$$

Substituting Eqn (3.17) and (3.18) into nine terms of Eqn (3.10) and splitting it into two terms, right hand side (RHS) and left hand side (LHS) for simplicity, one obtains

$$
\begin{aligned}
x_1F_1''''(\beta) &= 24x_1a_4 + \sum_{m=1}^{\infty} x_1(m+4)(m+3)(m+2)(m+1) \\
&\quad \times a_{m+1}(\beta-\beta_1)^m \\
x_2(\beta-\beta_1)F_1'''(\beta) &= \sum_{m=1}^{\infty} x_2(m+2)(m+1)ma_{m+2}(\beta-\beta_1)^m \\
x_3F_1'''(\beta) &= 6x_3a_3 + \sum_{m=1}^{\infty} x_3(m+3)(m+2)(m+1)a_{m+3}(\beta-\beta_1)^m \\
x_4(\beta-\beta_1)^2F_1''(\beta) &= \sum_{m=1}^{\infty} x_4m(m-1)a_m(\beta-\beta_1)^m \\
x_5(\beta-\beta_1)F_1''(\beta) &= \sum_{m=1}^{\infty} x_5(m+1)ma_{m+1}(\beta-\beta_1)^m \\
x_6F_1''(\beta) &= 2x_6a_2 + \sum_{m=1}^{\infty} x_6(m+2)(m+1)a_{m+2}(\beta-\beta_1)^m \\
x_7(\beta-\beta_1)F_1'(\beta) &= \sum_{m=1}^{\infty} x_7ma_m(\beta-\beta_1)^m \\
x_8F_1'(\beta) &= x_8a_1 + \sum_{m=1}^{\infty} x_8(m+1)a_{m+1}(\beta-\beta_1)^m \\
x_9F_1(\beta) &= x_9a_0 + \sum_{m=1}^{\infty} x_9a_m(\beta-\beta_1)^m \qquad (3.19)
\end{aligned}
$$

Summation of all terms from the right hand side (RHS) as well as from the left hand

side (LHS) of Eqn (3.19) is to be equal to 0. Summation of the first part of the first, third, sixth, eighth, and ninth term of right hand side (RHS) of Eqn (3.19) gives a relation between coefficients:

$$a_4 = \frac{1}{24x_1}(6x_3a_3 + 2x_6a_2 + x_8a_1 + x_9a_0) \tag{3.20}$$

Therefore, $a_5, a_6, ..., a_\infty$ can be formulated as,

$$\begin{aligned} a_{m+4} &= \frac{1}{s_{m+4}}\Big\{s_{m+3}a_{m+3} + s_{m+2}a_{m+2} + s_{m+1}a_{m+1} + s_m a_m\Big\} \\ m &= 1, 2, 3, ..., \infty \end{aligned} \tag{3.21}$$

where

$$\begin{aligned} s_{m+4} &= x_1(m+4)(m+3)(m+2)(m+1) \\ s_{m+3} &= x_3(m+3)(m+2)(m+1) \\ s_{m+2} &= x_2(m+2)(m+1)m + x_6(m+2)(m+1) \\ s_{m+1} &= x_5(m+1)m + x_8(m+1) \\ s_m &= x_4(m-1)m + x_7 m + x_9 \end{aligned}$$

In the numerical computations, the first four coefficients of $F_1(\mu, \beta)$ function, namely, a_0, a_1, a_2, a_3, can be obtained from the initial conditions (Eqn 3.12), which is in term

of the function $F_1(\beta_1)$ and its first three derivatives at initial time β_1, i.e.,

$$a_0 = F_1(\beta_1);\ a_1 = F_1^{'}(\beta_1);\ a_2 = \frac{1}{2}F_1^{''}(\beta_1);\ a_3 = \frac{1}{6}F_1^{'''}(\beta_1) \tag{3.22}$$

The coefficient, a_4, can be obtained from Eqn (3.20). Based on Eqn (3.21), the coefficients $a_5, a_6, ..., a_M$ in the series expansion of the solution can be easily computed. The same procedure is also used to find b_m and c_m, which are the coefficients of the series of F_2 and F_3 function solutions, respectively. Therefore, the solution of F_1, F_2 and F_3 functions can be summarized respectively as:

$$F_1(\mu, \beta) = \sum_{m=0}^{M_1} a_m(\beta - \beta_1)^m \tag{3.23}$$

$$F_2(\mu, \beta) = \sum_{m=0}^{M_2} b_m(\beta - \beta_1)^m \tag{3.24}$$

$$F_3(\mu, \beta) = \sum_{m=0}^{M_3} c_m(\beta - \beta_1)^m \tag{3.25}$$

where a_m, b_m and c_m are coefficients series, and, M_1, M_2 and M_3 are total expansion orders of series of F_1, F_2 and F_3 functions respectively. Finally $\tilde{F}(P, Q; t)$ and $\tilde{F}_n(P, Q; t)$ can be summarized respectively as:

$$\tilde{F}(P, Q; t) = C_1 \sum_{m=0}^{M_1} a_m(\beta - \beta_1)^m \tag{3.26}$$

$$\tilde{F}_n(P, Q; t) = \left(C_2.\vec{n}_{x_Q} + C_3.\vec{n}_{y_Q}\right) \sum_{m=0}^{M_2} b_m(\beta - \beta_1)^m$$

$$+C_4.\vec{n}_{z_Q}\sum_{m=0}^{M_3} c_m(\beta-\beta_1)^m \tag{3.27}$$

where,

$$\begin{aligned}
C_1 &= 2\sqrt{\frac{g}{r_{P\bar{Q}}^3}} \\
C_2 &= -2\sqrt{\frac{g}{r_{P\bar{Q}}^3}}\frac{x_Q-x_P}{r_{P\bar{Q}}R} \\
C_3 &= -2\sqrt{\frac{g}{r_{P\bar{Q}}^3}}\frac{y_Q-y_P}{r_{P\bar{Q}}R} \\
C_4 &= 2\sqrt{\frac{g}{r_{P\bar{Q}}^3}}\frac{1}{r_{P\bar{Q}}R}
\end{aligned}$$

3.3 The Computation of F_1, F_2, and F_3

The computational results of $F_1(\mu,\beta)$, $F_2(\mu,\beta)$, and $F_3(\mu,\beta)$ functions are plotted on Figures 3.1, 3.2, and 3.3 in domain $0 \leq \mu \leq 1;\ 0 \leq \beta \leq 12$, respectively.

Consider now the Power series expansion method, which was investigated, qualitatively. The accuracy and the computing time of the new approach depend on the time range $\Delta\beta$. The time range, $\Delta\beta = \beta - \beta_1$ is applied in order to speed up the convergence of the summation of an infinite series in numerical computation. The number of coefficients in the series is obtained for each time range determined. With the coefficients of series obtained, we can decide further any time step for simulation. This is shown in the sketch of Figure 3.4. The computational tests are conducted with different time range setup 0.5, 1, 1.5, 2 and 3, respectively in domain $0 \leq \beta \leq 15$ for μ equal to 0, 0.5 and 1, respectively. The results are shown in Tables 3.1, 3.2, and

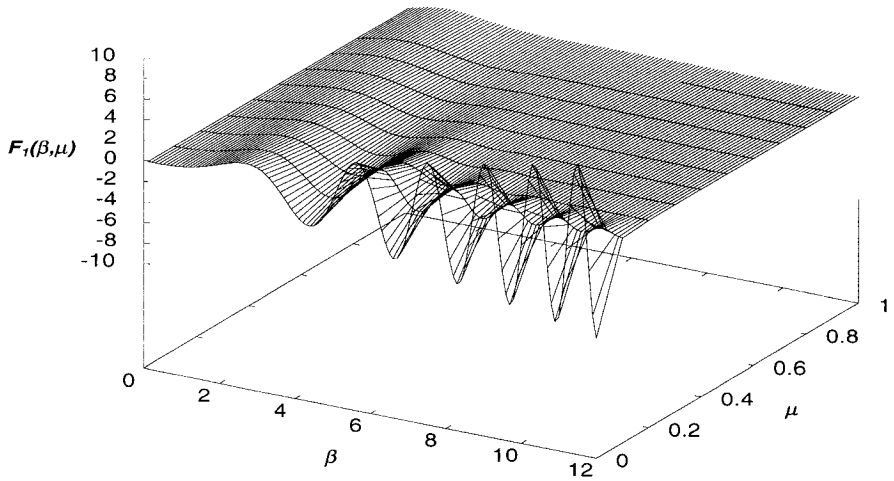

Figure 3.1: $F_1(\beta, \mu)$ function for $0 \leq \mu \leq 1,\ 0 \leq \beta \leq 12$

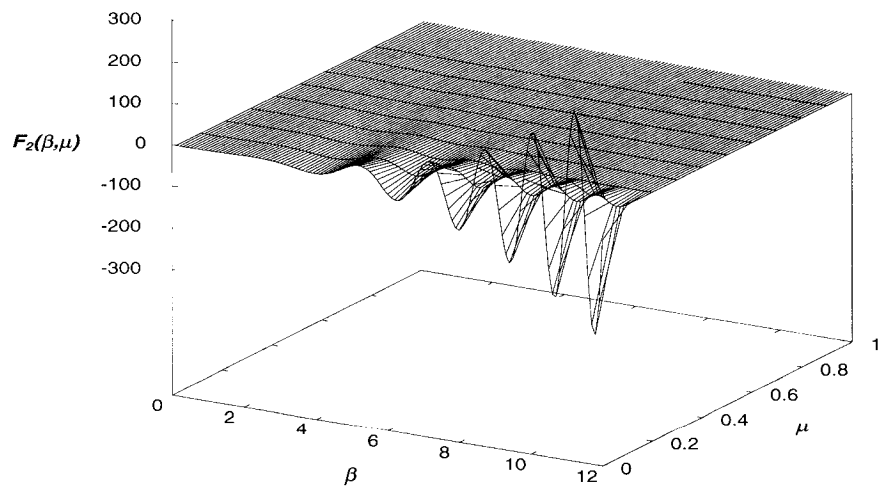

Figure 3.2: $F_2(\beta, \mu)$ function for $0 \leq \mu \leq 1,\ 0 \leq \beta \leq 12$

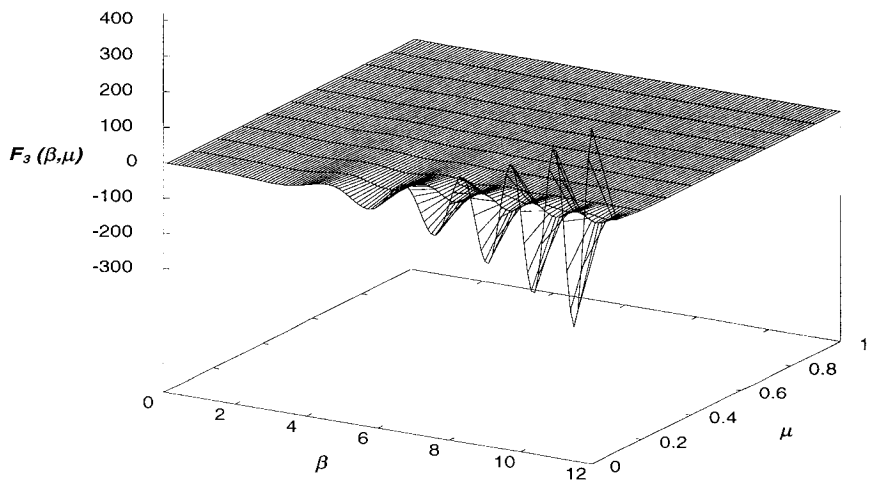

Figure 3.3: $F_3(\beta, \mu)$ function for $0 \leq \mu \leq 1,\ 0 \leq \beta \leq 12$

3.3 that list data in terms of the total expansion order, M_{ev}, of each time range and the root mean square (RMS) error evaluation, where RMS is defined as

$$RMS = \sqrt{\frac{1}{N}\sum_{j=1}^{N}\left(\phi^j_{\text{exact}} - \phi^j_{\text{num}}\right)^2} \tag{3.28}$$

where $(\phi^j_{\text{exact}} - \phi^j_{\text{num}})$ is the relative difference between successive partial sum of Eqn (3.19) equal to or less than 10^{-16}.

It is shown in Tables 3.1, 3.2 and 3.3 that due to the very small value of RMS error, the computed $F_1(\mu, \beta)$ function by the power series of Green's function is the analytical solution of Eqn (3.10). Also, the tables show, the best time range, $\Delta\beta$, might be equal to 0.5 with small error as well as total number of expansion order. This time range is used in the next computation of $F_1(\mu, \beta)$, $F_2(\mu, \beta)$, and $F_3(\mu, \beta)$ functions.

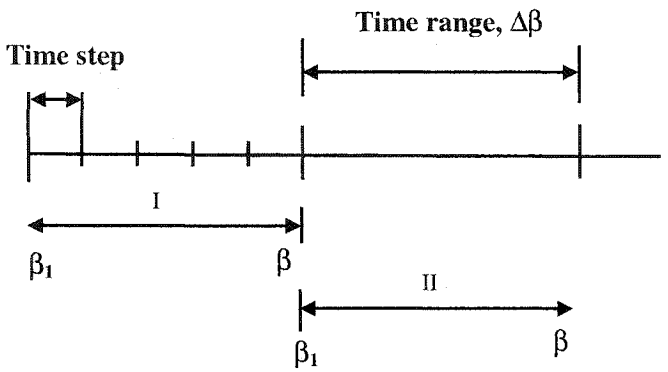

Figure 3.4: Time sketch

Table 3.1: The time range evaluation of $F_1(\mu, \beta)$ for $0 \leq \beta \leq 15$

Time range, $\Delta\beta$	$\mu = 0$		$\mu = 0.5$		$\mu = 1$	
	M_{ev}	RMS	M_{ev}	RMS	M_{ev}	RMS
0.5	32	1.00E-11	29	1.31E-15	24	1.54E-16
1.0	42	1.06E-10	38	2.22E-15	32	3.47E-16
1.5	51	1.04E-09	47	5.45E-15	38	1.06E-15
2.0	59	4.66E-07	55	2.66E-14	43	2.52E-15
3.0	75	3.71E-05	72	8.49E-13	58	2.45E-14

Table 3.2: The time range evaluation of $F_2(\mu, \beta)$ for $0 \leq \beta \leq 15$

Time range, $\Delta\beta$	$\mu = 0$		$\mu = 0.5$		$\mu = 1$	
	M_{ev}	RMS	M_{ev}	RMS	M_{ev}	RMS
0.5	32	6.56E-10	31	8.16E-15	0.0	0.00E+00
1.0	42	1.22E-08	40	1.14E-14	0.0	0.00E+00
1.5	53	6.65E-08	49	8.91E-14	0.0	0.00E+00
2.0	62	1.43E-05	59	3.86E-13	0.0	0.00E+00
3.0	78	4.25E-04	75	1.54E-11	0.0	0.00E+00

Table 3.3: The time range evaluation of $F_3(\mu, \beta)$ for $0 \leq \beta \leq 15$

Time range, $\Delta\beta$	$\mu = 0$		$\mu = 0.5$		$\mu = 1$	
	M_{ev}	RMS	M_{ev}	RMS	M_{ev}	RMS
0.5	32	6.04E-10	31	6.47E-15	25	1.73E-15
1.0	42	7.35E-09	40	1.73E-14	33	2.08E-15
1.5	51	3.26E-08	50	1.52E-13	39	5.46E-15
2.0	62	4.24E-05	58	3.22E-13	46	1.62E-14
3.0	77	1.95E-03	76	4.94E-11	62	1.55E-13

3.3.1 Analytical expression for $\mu = 0$

It is shown in Figures 3.1, 3.2 and 3.3 that when both the source, Q, and the field, P, lie on the free surface (i.e. $\mu = 0, z_P = z_Q = 0$), the function has oscillatory behavior. Eqns (3.3), (3.8), and (3.9) reduce to term of first kind Bessel functions, and the same expressions are given by Wehausen and Laitone (1960) as,

$$F_1(0,\beta) = \frac{\pi\beta^3}{16\sqrt{2}}\Big\{J_{\frac{1}{4}}\Big(\frac{\beta^2}{8}\Big)J_{-\frac{1}{4}}\Big(\frac{\beta^2}{8}\Big) + J_{\frac{3}{4}}\Big(\frac{\beta^2}{8}\Big)J_{-\frac{3}{4}}\Big(\frac{\beta^2}{8}\Big)\Big\} \tag{3.29}$$

$$\begin{aligned} F_2(0,\beta) = \frac{\pi\beta^3}{32\sqrt{2}}\Big\{5J_{\frac{1}{4}}\Big(\frac{\beta^2}{8}\Big)J_{-\frac{1}{4}}\Big(\frac{\beta^2}{8}\Big) + \frac{\beta^2}{2}\Big[J_{-\frac{1}{4}}\Big(\frac{\beta^2}{8}\Big)J_{-\frac{3}{4}}\Big(\frac{\beta^2}{8}\Big) \\ -J_{\frac{1}{4}}\Big(\frac{\beta^2}{8}\Big)J_{\frac{3}{4}}\Big(\frac{\beta^2}{8}\Big)\Big] + 3J_{\frac{3}{4}}\Big(\frac{\beta^2}{8}\Big)J_{-\frac{3}{4}}\Big(\frac{\beta^2}{8}\Big)\Big\} \end{aligned} \tag{3.30}$$

$$F_3(0,\beta) = -\frac{\pi\beta^3}{32\sqrt{2}}\Big\{\Big(\frac{8}{2\beta^2}-\frac{\beta^2}{2}\Big)J_{\frac{1}{4}}\Big(\frac{\beta^2}{8}\Big)J_{-\frac{1}{4}}\Big(\frac{\beta^2}{8}\Big) - 3\Big[J_{\frac{1}{4}}\Big(\frac{\beta^2}{8}\Big)J_{\frac{3}{4}}\Big(\frac{\beta^2}{8}\Big) - J_{-\frac{1}{4}}\Big(\frac{\beta^2}{8}\Big)J_{-\frac{3}{4}}\Big(\frac{\beta^2}{8}\Big)\Big] - \frac{\beta^2}{2}J_{\frac{3}{4}}\Big(\frac{\beta^2}{8}\Big)J_{-\frac{3}{4}}\Big(\frac{\beta^2}{8}\Big)\Big\} \quad (3.31)$$

The Bessel function of arbitrary order in Eqn (3.29), (3.30) and (3.31) can be solved numerically using recurrence relation with the series expansion for small arguments and an asymptotic expansion for large arguments, following Zhang and Jin (1996).

Therefore, in order to show how the accuracy of the new approach, the computation of the Power Series of Green function (PSGf) is validated by evaluating of the analytical expressions of $F_1(\beta,\mu)$, $F_2(\beta,\mu)$ and $F_3(\beta,\mu)$ in domain $\mu = 0$ and $0 \leq \beta \leq 15$, with a time step of 0.1. The results are plotted in Figures 3.5, 3.6, and 3.7 respectively.

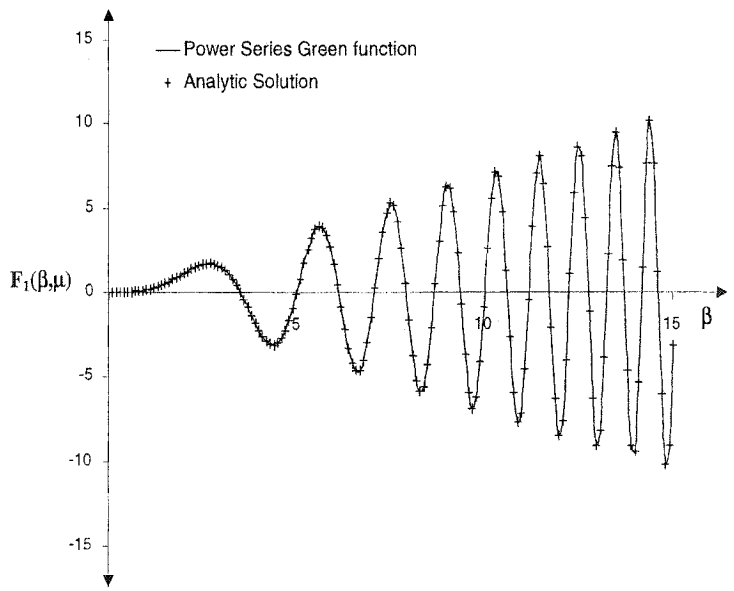

Figure 3.5: Comparison of $F_1(\beta,\mu)$ function for $\mu = 0,\ 0 \leq \beta \leq 15$, Time step= 0.1

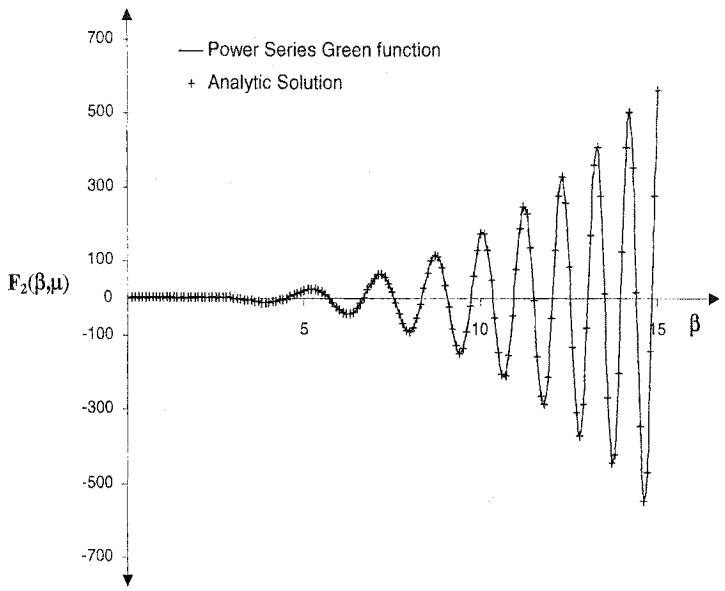

Figure 3.6: Comparison of $F_2(\beta, \mu)$ function for $\mu = 0,\ 0 \leq \beta \leq 15$, Time step $= 0.1$

3.3.2 Analytical expression for $\mu = 1$

When the field point, P, and the source point, Q, are at the same vertical axis which is $R = 0$, then μ is equal to 1. The Bessel function in Eqn (3.1) will disappear when $\mu = 1$, and the $F_1(\beta, \mu)$ function is expressed analytically as a confluent hypergeometric function given by Clément (1998a) such as

$$F_1(\beta, \mu) = \beta \exp\Big(-\frac{\beta^2}{4}\Big)\mathrm{M}\Big(-\frac{1}{2}, \frac{3}{2}, \frac{\beta^2}{4}\Big) \tag{3.32}$$

Equation (3.32) can be solved numerically using recurrence relation for confluent hypergeometric function following Zhang and Jin (1996). This analytical solution can be used to validate the accuracy of the power series Green's function for $F_1(\beta, \mu)$ evaluation at $\mu = 1$. The comparative results are plotted in Figure 3.8 at $0 \leq \beta \leq 15$

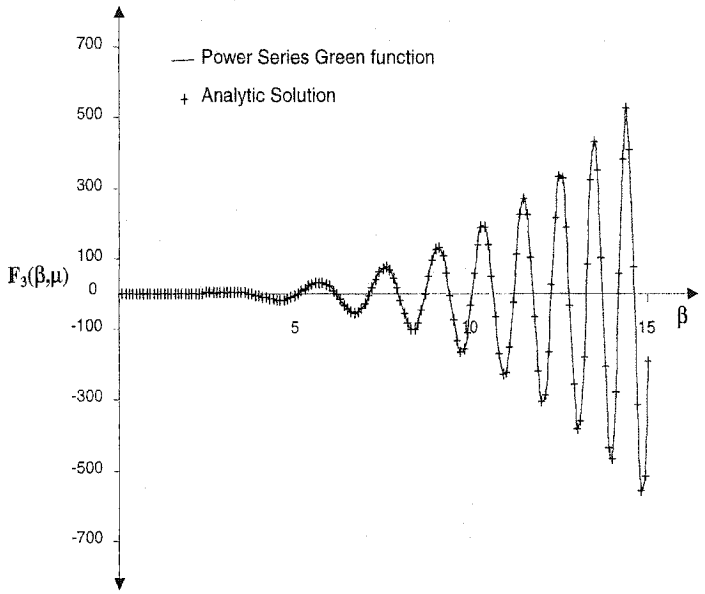

Figure 3.7: Comparison of $F_3(\beta, \mu)$ function for $\mu = 0,\ 0 \leq \beta \leq 15$, Time step $= 0.1$

with a time step of 0.1.

Now, we compare the proposed method to other methods such as the fifth-order Runge-Kutta method and tabulation method developed by Huang and Hsiung (1996). The numerical comparison is presented in Table 3.4 in terms of Root Mean Square (RMS) error for different time step, 0.1, 0.05, and 0.01, respectively. The RMS error evaluation is used to measure the accuracy of numerical computational, and it can be defined as:

$$RMS = \sqrt{\frac{1}{N}\sum_{j=1}^{N}\left\{\frac{F_{\text{exact}}^{(j)} - F_{\text{num}}^{(j)}}{F_{\text{exact}}^{(j)}}\right\}^2} \tag{3.33}$$

It is shown in Table 3.4 that a power Series of Green's function gives better

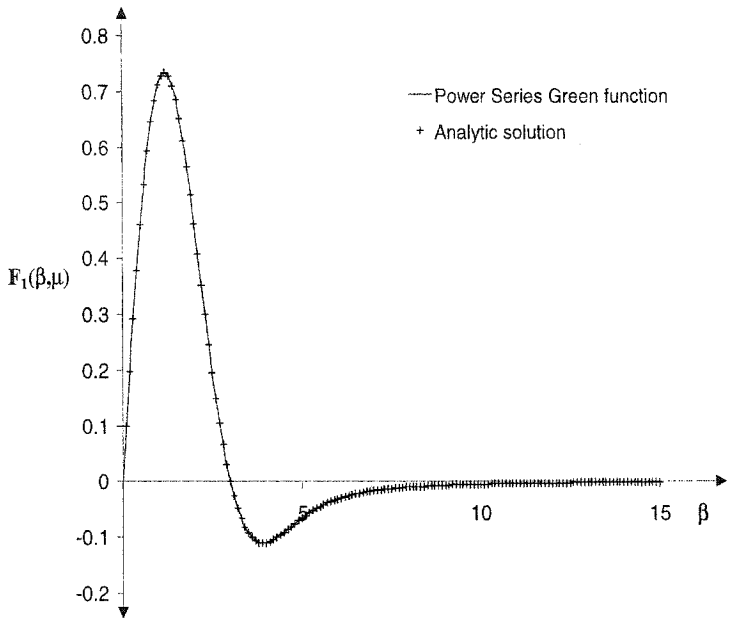

Figure 3.8: Comparison of $F_1(\beta, \mu)$ function for $\mu = 1,\ 0 \leq \beta \leq 15$, Time step $= 0.1$

Table 3.4: The RMS error for $F_1(\mu, \beta)$ evaluation at $0 \leq \beta \leq 15$

Time step	$\mu = 0$			$\mu = 1$		
	PSGf	RK-05	Tabulation	PSGf	RK-05	Tabulation
0.1	9.89E-13	0.01197	6.13E-06	5.98E-12	0.00628	0.00032
0.05	9.89E-13	0.01193	6.13E-06	4.26E-12	0.00449	0.00060
0.01	9.89E-13	0.01191	1.28E-05	2.50E-12	0.00263	0.00420

accuracy compared to a fifth-order Runge-Kutta method or the tabulation method. In evaluating with a power series of Green's function, reducing the time step of numerical computation does not much improve accuracy since the time range $\Delta\beta$ is fixed. This differs from the common numerical method such as Runge-Kutta, where numerical errors decrease with decreasing time step. The investigation of the tabulation method (3.4) shows that the error increases when the time step is increased. The time step used on tabulation is 0.1, and the errors originate from interpolation.

3.4 The Convolution Integral Evaluation

In Eqn (2.25), two convolution integrals have to be evaluated on the right hand side. The major part of the total CPU time requirement in the numerical computation of (2.25) is to evaluate the convolution integral, which is the memory part of Green's function equation, $\tilde{F}$. The function $\tilde{F}$ has to be evaluated for each location of the couple points P and Q on the body surface at every time step, and also be stored for the next time-step evaluation. In this section a power series of Green's function is applied to evaluate the convolution integrals and a computational test is conducted to compare the accuracy of this approach to others. Let us rewrite both convolution integrals of Eqn (2.25) in the form of

$$I(P,Q,t) = \int_0^t q(Q,t_1)\tilde{F}(P,Q;t-t_1)dt_1 \tag{3.34}$$

$$J(P,Q,t) = \int_0^t \phi(Q,t_1)\tilde{F}_{n_Q}(P,Q;t-t_1)dt_1 \tag{3.35}$$

where $\tilde{F}(P,Q,t)$ and $\tilde{F}_{n_Q}(P,Q,t)$ are expressed in Eqn (3.26) and (3.27), respectively. The terms $q(Q,t_1)$ and $\phi(Q,t_1)$ are body boundary condition and a previous velocity potential on body surface, respectively. Because $q(Q,t_1)$ and $\phi(Q,t_1)$ are not continuous, Eqn (3.35) and (3.35) might be solved numerically. Currently, there are several methods available to evaluate convolution integral, and Trapezoid rule is the most commondly used. The linear variation approach proposed by Kashiwagi (2000) is used in order to keep numerical acuracy. By analytical derivation, we conclude Eqn (3.35) and (3.35) can be performed numerically as,

$$I(L\Delta t) = \sum_{l=0}^{L-1} \frac{\Delta t}{6}\Big\{(q_l + 2q_{l+1})\tilde{F}_{L-(l+1)} + (q_{l+1} + 2\phi_l)\tilde{F}_{L-1}\Big\} \tag{3.36}$$

$$J(L\Delta t) = \sum_{l=0}^{L-1} \frac{\Delta t}{6}\Big\{(\phi_l + 2\phi_{l+1})F_{n_{L-(l+1)}} + (\phi_{l+1} + 2\phi_l)F_{n_{L-1}}\Big\} \tag{3.37}$$

where Δt is a constant time-step size, and $t = L\Delta t$ is the present time. The evaluation of system output $I(P, Q; t)$ and $J(P, Q; t)$ with the input $q(t)$ and $\phi(t)$ respectively which are assumed equal to $\sin(6t)$ are performed. However, the analytical solution of Eqn (3.35) and (3.35) have to be developed in order to validate the numerical approaches.

The analytic solution of the Eqn (3.35) can be performed by substituting an alternative solution of $\tilde{F}$ function presented in Eqn (3.26) into Eqn (3.35) yields,

$$I(P, Q; t) = \sum_{m=0}^{M_1} a_m(P, Q) \int_0^t \sin(6\tau)(t - t_1)^m d\tau \tag{3.38}$$

Because $q(Q, t_1)$ is a continuous equation, by using the recursive relation, Eqn (3.38) can be solved analytically as,

$$I_m(P, Q; t) = \sum_{m=1}^{M_1} a_m(P, Q) n_z \Big[\frac{t^m}{6} - \frac{m}{6}\int_0^t (\cos(6t_1)(t - t_1)^{m-1} dt_1\Big] \tag{3.39}$$

$$II_m(P, Q; t) = \sum_{m=1}^{M_1} a_m(P, Q) n_z \Big[\frac{m}{6}\int_0^t (\sin(6t_1)(t - t_1)^{m-1} dt_1\Big] \tag{3.40}$$

and it can be simplified as,

$$I_m(P,Q;t) = \sum_{m=1}^{M_1} a_m(P,Q)n_z\Big[\frac{t^m}{6} - \frac{m}{6}II_{m-1}\Big] \tag{3.41}$$

$$II_m(P,Q;t) = \sum_{m=1}^{M_1} a_m(P,Q)n_z\Big[\frac{m}{6}I_{m-1}\Big] \tag{3.42}$$

with initial condition as

$$I_0(P,Q;0) = -\frac{1}{6}(\cos(6t) - 1) \tag{3.43}$$

$$II_0(P,Q;0) = \frac{1}{6}(\sin(6t)) \tag{3.44}$$

At this point, computational tests for convolution integrals are presented. Numerical tests are performed on a field point $P(5,0,-1)$ and a source point $Q(2,0,-1)$ in the $0 \leq t \leq 20$ domain, conducted with different time steps, ($\Delta t = 0.005,\ 0.01,\ 0.05$ and 0.1 respectively). The advantages of the new approach are demonstrated by comparing with the Runge-Kutta method, and the tabulation method developed by Huang and Hsiung (1996). Power series of Green's function (PSGf) with the extended linear variation is compared with the fifth-order Runge-Kutta method and the tabulation method, both combined with the trapezoidal rule in evaluating Eqn (3.35). The results are plotted in Figure 3.9, and the numerical performance data (elapsed time (ET) and root mean square (RMS) error) are presented in Table 3.5.

The elapsed time (ET) is a measure of the amount of time that has passed since the program started. Elapsed time is usually close to the CPU time if the computer spent the vast majority of its time executing the program. Elapsed time is evaluated by setting the record time function at the start and end of the program, and subtracting

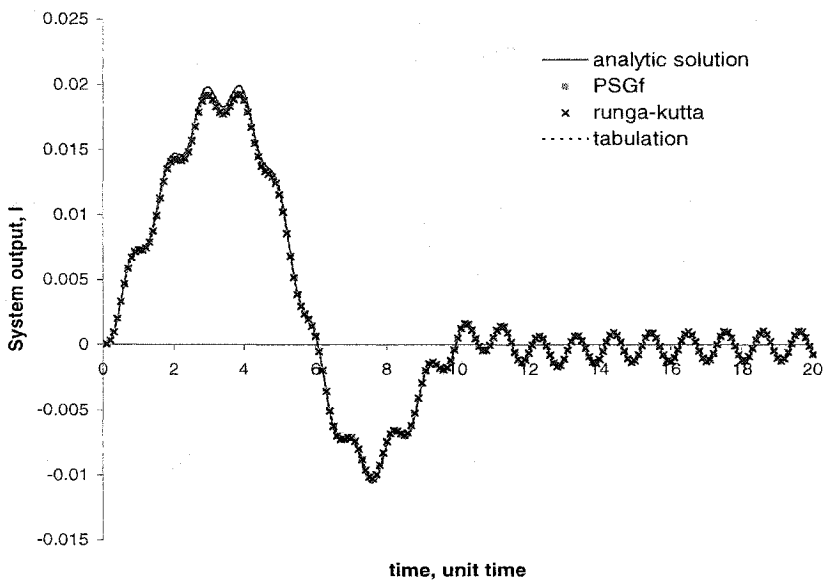

Figure 3.9: System output for $P(5, 0, -1)$, $Q(2, 0, -1)$, $0 \leq t \leq 20$, $\Delta t = 0.1$

the former from the latter. (This program was run on a PC Pentium 1 Gb Mhz, 256 RAM).

Figure 3.9 and Table 3.5 illustrate the superiority of PSGf compared to the Runge-Kutta method or tabulation method, especially when the time-step is decreased. Although the RMS error for PSGf and Runge-Kutta appears almost indistinguishable at time step of $\Delta t = 0.1$ and $\Delta t = 0.05$, the result at $\Delta t = 0.01$ shows the RMS error for Runge-Kutta almost three times that of PSGf, and the elapsed times three to five times greater.

Table 3.5: Numerical performances of the convolution integral evaluation

Time step	PSGf with linear variation		RK-O5 with trapezoid rule		Tabulation with trapezoid rule	
	ET	RMS	ET	RMS	ET	RMS
0.1	0.0156	0.0308	0.8120	0.0306	1.7344	0.0775
0.05	0.0625	0.0079	1.3910	0.0079	3.0469	0.07158
0.01	1.3281	0.0009	7.2960	0.0023	44.5000	0.0087
0.005	5.1719	0.0008	15.406	0.0023	176.1875	0.0082

Chapter 4

Numerical Implementation

In this section, a one-panel method to evaluate Eqn (3.1) is proposed. In this method, the body surface is obtained as one panel, and the number of Gaussian quadrature points are generated on the surface body. The Gaussian quadrature points, which are used also as collocation points, are calculated exactly from the mathematical surface definition of the body, and the potential distribution are determined at these points. Since there are no exact mathematical surface available for the irregular shape of body like ship, submarine, offshore structure etc., the NURBS (Non-Uniform Rational B-Spline) is adopted in order to generate the body surface mathematically.

After discretized the body surface into a number of Gaussian points, the singularity of the boundary integral in term of the potential distribution is regularized based on regularized Green's formula introduced by Landwaber and Macagno (1969). In order to simplify the solution, the discretized integral is decomposed into a linear system of algebraic equations with two kernel matrices, $[G]$ and $[H]$, and the Gaussian elimination method is used to solve the simulataneous equations to obtain unknown potentials at $t = 0$. The time integral of the boundary integral equation have to be solved by using the time-stepping approach. The memory part of the Green's function

and its normal are computed at each time step and these quantities are stored in the computer memory for use in the convolution term at subsequent times. The convolution integrals involved in the boundary integral are evaluated by a linear variation approach.

4.1 Discretization of Body Surface

Both the analytical surface and the NURBS surface procedures are employed to construct the sphere and ellipsoid surfaces respectively.

4.1.1 The Analytical Surface

The exact surface definition of an 3-D Sphere is used to generate gaussian quadrature points, which are also called collocation points. The potential, ϕ, is assumed constant and it is determined at each collocation point. There are two parameters, θ and φ, which are used to locate collocation points on the surface of the sphere so that the Jacobians are dependent on the collocation points. Considering a half body of the sphere, the parameters θ and φ are divided into segments, $0 \leq \theta \leq 2\pi$ and $0 \leq \varphi \leq \pi$, respectively. The collocation points of the sphere with a radius, r, are obtained by,

$$\begin{aligned} x_{ij} &= r\cos\theta \\ y_{ij} &= r\sin\theta\cos\varphi \\ z_{ij} &= -r\sin\theta\sin\varphi \end{aligned} \tag{4.1}$$

The gauss-legendre quadrature with 8 and 16 points are used, and the total number of collocation points for a half suface body is 8 x 8 = 64 and 16 x 16 = 256 respectively, and its shown in Figure 4.1.

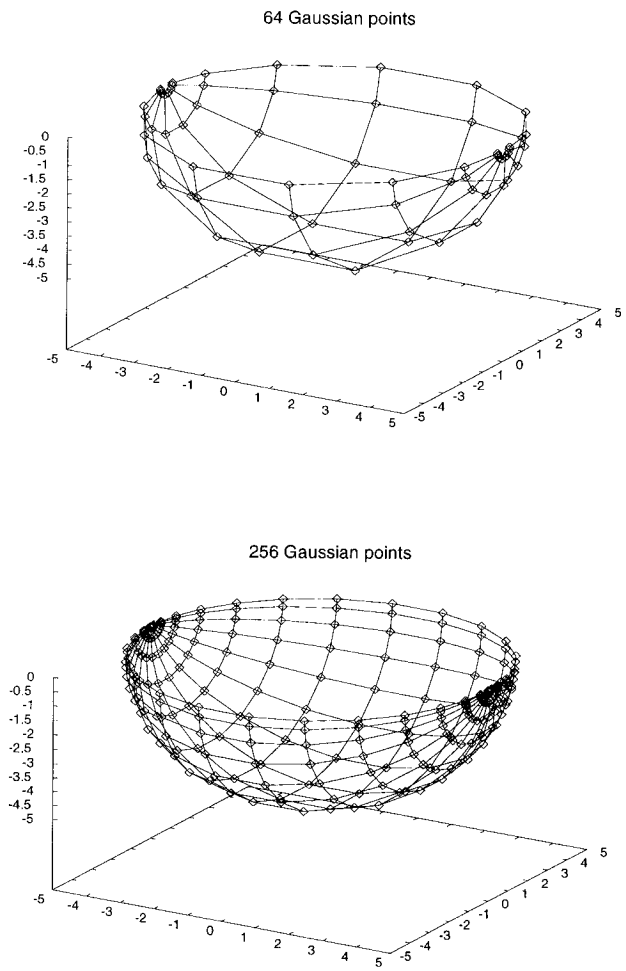

Figure 4.1: Hemisphere Gaussian quadrature points

4.1.2 NURBS (Non-Uniform Rational B-Spline)

The body can be generated by NURBS surface based on the offset data as input, and the following procedure is inspired by Sheng's work (2003). The NURBS surface is given as:

$$\vec{W}(u,v) = \frac{\sum_{i=0}^{n}\sum_{j=0}^{m}\omega_{i,j}N_{i,p}(u)N_{i,q}(v)\vec{A}_{i,j}}{\sum_{i=0}^{n}\sum_{j=0}^{m}\omega_{i,j}N_{i,p}(u)N_{i,q}(v)} \tag{4.2}$$

where $\vec{W}(u,v)$ is the position vector along the the NURBS surface, $A_{i,j}$ is control point located at $(X_{i,j}, Y_{i,j}, Z_{i,j})$ associated with weight $\omega_{i,j}$. $N_{i,p}(u)$ and $N_{j,q}(v)$ are the basis functions of degrees p and q in u and v direction, respectively. The value of the parameters u and v varies from 0 to 1.

The control points, $\vec{A}_{i,j}$ for $i = 1, ..., n$ and $j = 1, ..., m$, in Eqn (4.2) can be defined, if the offset data points, $W_{k,l}$, for $k = 0, ..., n$ and $l = 0, ..., m$, on the curve surface are given. The nonuniform knot vectors, U and V have to be defined in order to compute the basis functions, $N_{i,p}(u)$ and $N_{j,q}(v)$. Detailed description to find the basis functions are presented by Piegl and Tiller (1997). Therefore, a system of two linear functions is developed to solve Eqn (4.2) obtaining control points $\vec{A}_{i,j}$.

Based on the number of control points, the weighting function, $w_{i,j}$, is defined by Legendre quadrature following Golub and Welsch (1969). Therefore, using Eqn (4.2), the new points, $\vec{W}'(x,y,z)$, on the NURBS surface of the new body, which are also obtained as Gaussian points or collocation points, can be determined based on the parameters u and v in which the number of points is adjustable. Three equations to find the coordinate x, y, z can be expressed as,

$$\begin{aligned} x = x(u,v) &= B(u,v)X_{i,j} \\ y = y(u,v) &= B(u,v)Y_{i,j} \\ z = z(u,v) &= B(u,v)Z_{i,j} \end{aligned} \tag{4.3}$$

where

$$B(u,v) = \frac{\sum_{i=0}^{n}\sum_{j=0}^{m}\omega_{i,j}N_{i,p}(u)N_{i,q}(v)}{\sum_{i=0}^{n}\sum_{j=0}^{m}\omega_{i,j}N_{i,p}(u)N_{i,q}(v)}$$

The unit normal vector of the $\vec{W}'$ is defined by the cross product of two unit tanget vectors in u and v directions such as

$$\vec{n} = n_x\vec{i} + n_y\vec{j} + n_z\vec{k} = \vec{d} \times \vec{e} \tag{4.4}$$

where the unit tangent vector $\vec{d}$ and $\vec{e}$ are

$$\vec{d} = \frac{1}{\left|\vec{S}_u\right|}\left[\frac{\partial x}{\partial u}\vec{i} + \frac{\partial y}{\partial u}\vec{j} + \frac{\partial z}{\partial u}\vec{k}\right] = d_x\vec{i} + d_y\vec{j} + d_z\vec{k} \tag{4.5}$$

$$\vec{e} = \frac{1}{\left|\vec{S}_v\right|}\left[\frac{\partial x}{\partial v}\vec{i} + \frac{\partial y}{\partial v}\vec{j} + \frac{\partial z}{\partial v}\vec{k}\right] = e_x\vec{i} + e_y\vec{j} + e_z\vec{k} \tag{4.6}$$

and

$$\begin{aligned} \left|\vec{S}_u\right| &= \sqrt{\left(\frac{\partial x}{\partial u}\right)^2 + \left(\frac{\partial y}{\partial u}\right)^2 + \left(\frac{\partial z}{\partial u}\right)^2} \\ \left|\vec{S}_v\right| &= \sqrt{\left(\frac{\partial x}{\partial v}\right)^2 + \left(\frac{\partial y}{\partial v}\right)^2 + \left(\frac{\partial z}{\partial v}\right)^2} \end{aligned}$$

therefore,

$$n_x = d_y e_z - d_z e_y, \quad n_y = d_z e_x - d_x e_z, \quad n_z = d_x e_y - d_y e_x \tag{4.7}$$

The Jacobian, J can be obtained as

$$J = \left|\vec{S}_u \times \vec{S}_v\right| \tag{4.8}$$

and for integral equation solution the weighting function including jacobian can be simplified as,

$$J_w = \frac{\omega_{i,j} J}{4} \tag{4.9}$$

In order to illustrate the accuracy of the geometric approximation of NURBS surface, the body surface of an ellipsoid, which is described mathematically below, can be taken into consideration,

$$\frac{x^2}{\bar{a}^2} + \frac{y^2}{\bar{b}^2} + \frac{z^2}{\bar{c}^2} = 1 \tag{4.10}$$

In the above equation, the parametric form in term of l_e and θ are presented as

$$x = l_e, \qquad y = \frac{\bar{b}}{\bar{a}}\sqrt{\bar{a}^2 - l_e^2}\cos\theta, \qquad z = \frac{\bar{c}}{\bar{a}}\sqrt{\bar{a}^2 - l_e^2}\sin\theta \tag{4.11}$$

with $-\bar{a} \leq l_e \leq \bar{a}$ and $\pi \leq \theta \leq 2\pi$. The half ellipsoids having length to beam ratio, $\bar{a}/\bar{b} = 4$ with two different draft which are the half length to draft ratio $\bar{a}/\bar{c}$ as $H = 4$ and 2 are used in numerical computation. Using the NURBS surface, the collocation points with weighting function including Jacobian can be generated based on the offset data. The number of collocation points can be adjusted considering with the time consuming and the accuracy of numerical computation. Figure 4.2 shows two different ellipsoids with $\bar{a} = 5$ in 16 x 16 gaussiant points.

The accuracy of NURBS surface compared to the exact geometry is shown in Table 4.1 in term of root mean square (RMS) error for different number of Gaussian points. The RMS can be obtained as

$$RMS = \sqrt{\frac{1}{n \times m}\sum_{i=1}^{n}\sum_{j=1}^{m}\left(\frac{z_{i,j}^{(exact)} - z_{i,j}^{(nurbs)}}{z_{i,j}^{(exact)}}\right)^2} \tag{4.12}$$

where n and m are the number of gaussiant point in x and y coordinate system respectively, and $z_{i,j}^{(exact)}$ is exact coordinate obtained from Eqn (4.10) based on NURBS coordinate $x_{i,j}^{(nurbs)}$ and $y_{i,j}^{(nurbs)}$ where it is described as

$$z_{i,j}^{(exact)} = \pm\bar{c}\sqrt{1 - \left(\frac{x_{i,j}^{(nurbs)}}{\bar{a}}\right)^2 - \left(\frac{y_{i,j}^{(nurbs)}}{\bar{b}}\right)^2} \tag{4.13}$$

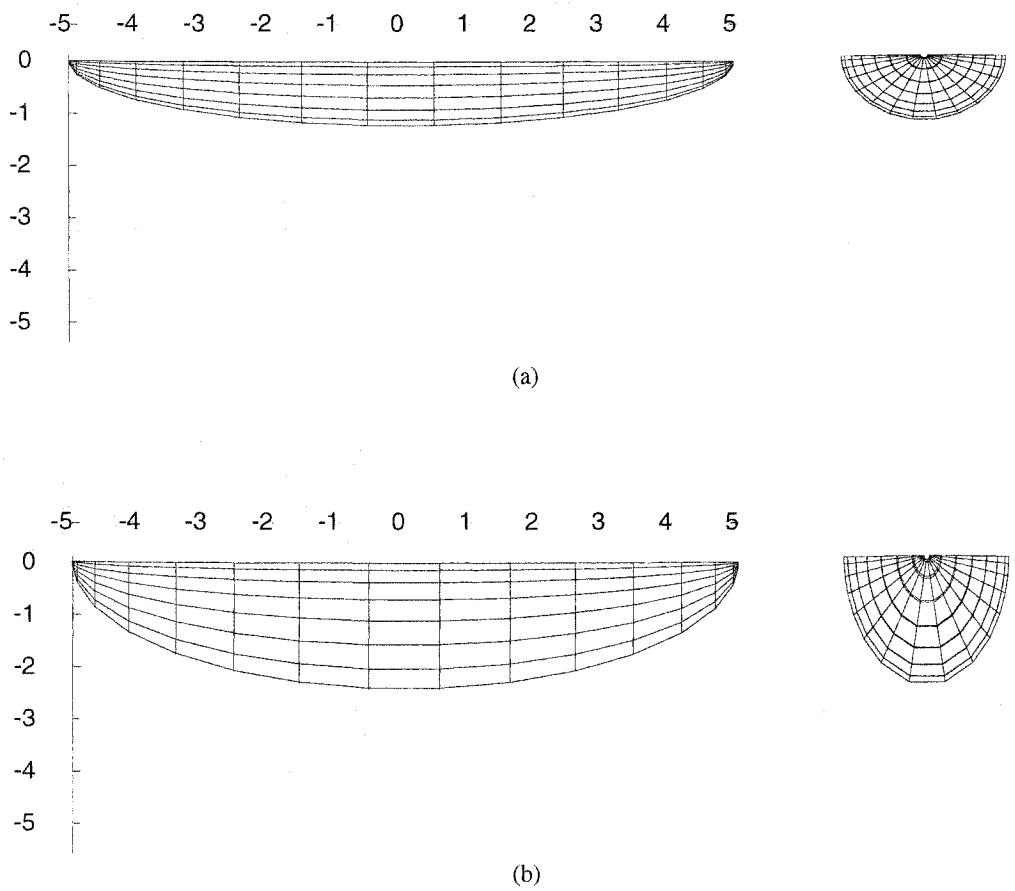

Figure 4.2: Ellipsoid generated by NURBS with $\frac{\bar{a}}{\bar{b}} = 4$, and (a) H = 4 (b) H = 2

Table 4.1: The accuracy of NURBS surface due to exact geometry

	RMS Error with different Gaussian points					
	8×8	12×8	12×12	16×16	32×32	64×64
H = 4	0.04370	0.0080	0.00372	0.00080	0.00011	0.000002
H = 2	0.01243	0.01269	0.00286	0.0079	0.00120	0.00003

4.2 Discretization of Integral Equation

After discretization of the body surface by Analytical or NURBS surface, the unknown potential distribution, ϕ, is computed by assuming a constant potential over each Gaussian point. This means the number of unknown potentials are the same as the number of Gaussian points over this body. The integral equation, Eqn (2.25), therefore can be simplified into a system of algebraic equations, convenient for solving the unknown potential. Since the body motions started from rest, a linear system must be factored twice, once at $t = 0$ and once at $t > 0$. These are the singularity integral and the free-surface integral to be evaluated respectively.

4.2.1 Discretization of Singularity Integral

The Eqn (2.33) can be discretized into a linear system of algebraic equations, and it is expressed in a matrix form as

$$[H][\phi] = [G][q] \tag{4.14}$$

where

$$
\begin{aligned}
H_{ii} &= 2 - \frac{\vec{r}_{ii'}.\vec{n}_i}{2\pi r_{ii'}^3} J_{w_i} - \sum_{j=1,j\neq i}^{N} \Big(\frac{\vec{r}_{ij}.\vec{n}_j}{2\pi r_{ij}^3} + \frac{\vec{r}_{i'j}.\vec{n}_j}{2\pi r_{i'j}^3} \Big) J_{w_j} \qquad \text{for } i = j \\
H_{ij} &= \sum_{j=1,j\neq i}^{N} \Big(\frac{\vec{r}_{ij}.\vec{n}_j}{2\pi r_{ij}^3} - \frac{\vec{r}_{ij'}.\vec{n}_j}{2\pi r_{ij'}^3} \Big) J_{w_j} \qquad \text{for } i \neq j \\
G_{ii} &= \frac{\phi_e}{2\pi\delta_i} + \frac{1}{\pi r_{ii'}} J_{w_j} + \sum_{j=1;j\neq i}^{N} \frac{\delta_j}{\delta_i} \Big(\frac{1}{2\pi r_{ij}} + \frac{1}{2\pi r_{ij'}} \Big) J_{w_j} \qquad \text{for } i = j \\
G_{ij} &= \sum_{j=1,j\neq i}^{N} \Big(\frac{1}{r_{ij}} + \frac{1}{r_{ij'}} \Big) J_{w_j} \qquad \text{for } i \neq j \\
q_j &= n_{k_j} \qquad \text{for } k = 1, 2, ..., 6 \\
&= \vec{r} \times n_{k_j} \\
\phi_j &= \phi_{k_j} \qquad \text{for } k = 1, 2, ..., 6
\end{aligned}
\tag{4.15}
$$

where N is the number of Gaussian points and J_w denotes the generalized Jacobian which includes a weighting function and differential area at the collocation point. The integral equation of δ function, Eqn (2.34), can be discretized by using Gaussian quadrature and decomposed into a linear system of algebraic equations as,

$$
[\delta^{(l+1)}] = [A][\delta^{(l)}] \tag{4.16}
$$

where

$$
\begin{aligned}
A_{ii} &= 1 - \sum_{j=1,j\neq i}^{N} \left(\frac{\vec{r}_{ij}.\vec{n}_j}{r_{ij}^3} + \frac{\vec{r}_{i'j}.\vec{n}_j}{r_{i'j}^3} \right) J_{w_j} \qquad \text{for } \; i = j \\
A_{ij} &= \sum_{j=1,j\neq i}^{N} \left(\frac{\vec{r}_{ij}.\vec{n}_i}{r_{ij}^3} + \frac{\vec{r}_{i'j}.\vec{n}_i}{r_{i'j}^3} \right) J_{w_j} \qquad \text{for } \; i \neq j
\end{aligned}
$$

$$r_{ij} = (x_j - x_i)\vec{i} + (y_j - y_i)\vec{j} + (z_j - z_i)\vec{k}$$
$$r_{i'j} = (x_j - x_i)\vec{i} + (y_j - y_i)\vec{j} + (z_j + z_i)\vec{k}$$

4.2.2 Discretization of Free-Surface Integral Equation

The equation (2.25) which involves the free-surface of Green's function, can be discretized by number of Gaussian points N, reducing it to a linear system of algebraic equations, which may be solved directly at each time step. The linear variation approach is used to carry out the convolution integral. The discrete form which must be solved at each time-step, L, up to the last time L_T. The linear simulataneous equations which must be solved are:

$$\left[H\right]\left[\phi^{t_L}\right] = \left[G\right]\left[q\right] + \left[G_a\right] - \left[G_b\right] \tag{4.17}$$

where matrix $[H]$, $[G]$, and $[q]$ are obtained on Eqn (4.15), and matrix $\left[G_a\right]$ and $\left[G_b\right]$ are calculated as

$$G_{a_j} = \frac{1}{2\pi}\sum_{l=0}^{L-1}\frac{\Delta t}{6}\left\{\left[F^{t_{L-(l+1)}}\right] + \left[F^{t_{L-l}}\right]\right\}\left[q\right] \tag{4.18}$$
$$G_{b_j} = -\frac{1}{2\pi}\sum_{l=0}^{L-l}\frac{\Delta t}{6}\left\{\left[\phi^{t_l} + 2\phi^{t_{l+1}}\right]\left[F_n^{t_{L-(l+1)}}\right] + \left[\phi^{t_{l+1}} + 2\phi^{t_l}\right]\left[F_n^{t_{L-l}}\right]\right\}$$

The matrix $[F^t]$ and $[F_n^t]$ are performed as,

$$
\begin{aligned}
F_{ij}^{t} &= \sum_{i=j=1}^{N} \sum_{m=0}^{M_1} a_{i,j}^{m} (t - t_1)^m J_{w_j} \\
F_{n_{ij}}^{t} &= \sum_{i=j=1}^{N} \Big\{ \sum_{m=0}^{M_2} b_{i,j}^{m} \Big(\frac{(x_j - x_i)}{R_{ij}} n_{x_j} + \frac{(y_j - y_i)}{R_{ij}} n_{y_j} \Big) + \sum_{m=0}^{M_3} c_{i,j}^{m} n_{z_j} \Big\} \\
&\quad \times (t - t_1)^m J_{w_j} \\
R_{ij} &= (x_j - x_i)\vec{i} + (y_j - y_i)\vec{j}
\end{aligned}
\tag{4.19}
$$

where $a_{i,j}^{m}, b_{i,j}^{m}$ and $c_{i,j}^{m}$ are the coefficient series, M_1, M_2 and M_3, are total expansion orders of series, and t is time stepping up to L_T. The summary of the numerical scheme is explained in term of flowchart system in Appendix C.

Chapter 5

Numerical Results

The numerical method described in the previous chapter is now compared to a series of analytical as well as numerical results. The results obtained by the present method are validated against those of the classical analytical results. They are also compared to other numerical computation results for a floating sphere, and semi-analytic results for a floating ellipsoid.

5.1 A Sphere

The first set of numerical results are obtained by using the power series Green's function added mass and damping coefficients on the floating hemisphere studied by Hulme (1982). Hulme found the analytical solution to the radiation of waves for floating half-submerged sphere in infinitely deep water by constructing an expansion for the velocity potential in terms of a series of spherical harmonics. This study evaluate numerically the added-mass and damping coefficients in heave and surge motion that Hulme determined analytically. Hulme's analytical results at zero forward speed provide the first benchmark of the present method.

The heaving added-mass coefficient, A_{33} in the frequency domain is transformed using Eqn (2.51) from the impulsive response, K_{33}. The damping coefficient in frequency domain is obtained using Eqn (2.52) with neglecting zero time condition. Figure 5.1 represents the heaving added-mass coefficient, A_{33}, computed by the present method and compared to Hulme's result. As the comparison curve shows, the present method gives a very good agreement with the analytical result. Comparison of the heaving damping coefficient, B_{33} presented in Figure 5.2 further validates the new method.

Figure 5.3 shows the surging added-mass coefficient obtained by the new method, compared to Hulme's analytical solution for a floating sphere. In the same floating body case, the surging damping coefficient is again determined by the new method and is analytically presented in Figure 5.4. The comparison between Figure 5.3 and Figure 5.4 shows that the computational results of the new method are very close to the analytical solution.

The non-dimensional response function for a floating sphere in heave and surge motion were also computed. Numerical result, which is conducted by Cohen (1986), is used as the second benckmark of the present method.

Figure 5.5 shows the non-dimensional memory function $K_{33}(t)\sqrt{r/g}/\rho\Delta$ for a floating sphere due to impulsive heave versus non-dimensional time $t\sqrt{r/g}$. In the present method, 8×8 and 12×8 gaussian points are generated by the NURBS on a half sphere. The agreement between Cohen's result and the calculation of the new method is excellent.

The same comparison is also presented in Figure 5.6 for non-dimensional memory function due to impulsive surge $K_{11}(t)\sqrt{r/g}/\rho\Delta$ for various non-dimensional times $t\sqrt{r/g}$. Numerical results of Power Series of Green's function compare very well with Cohen's results (1986).

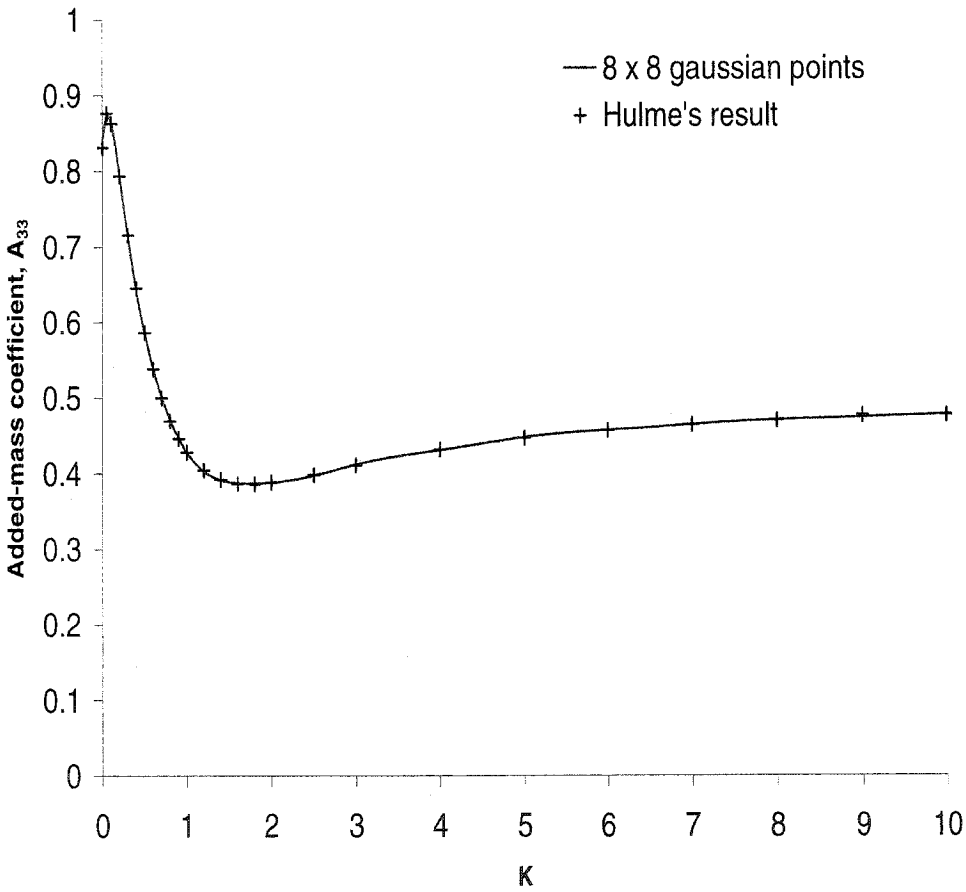

Figure 5.1: Added mass coefficient in heave motion of a floating Sphere

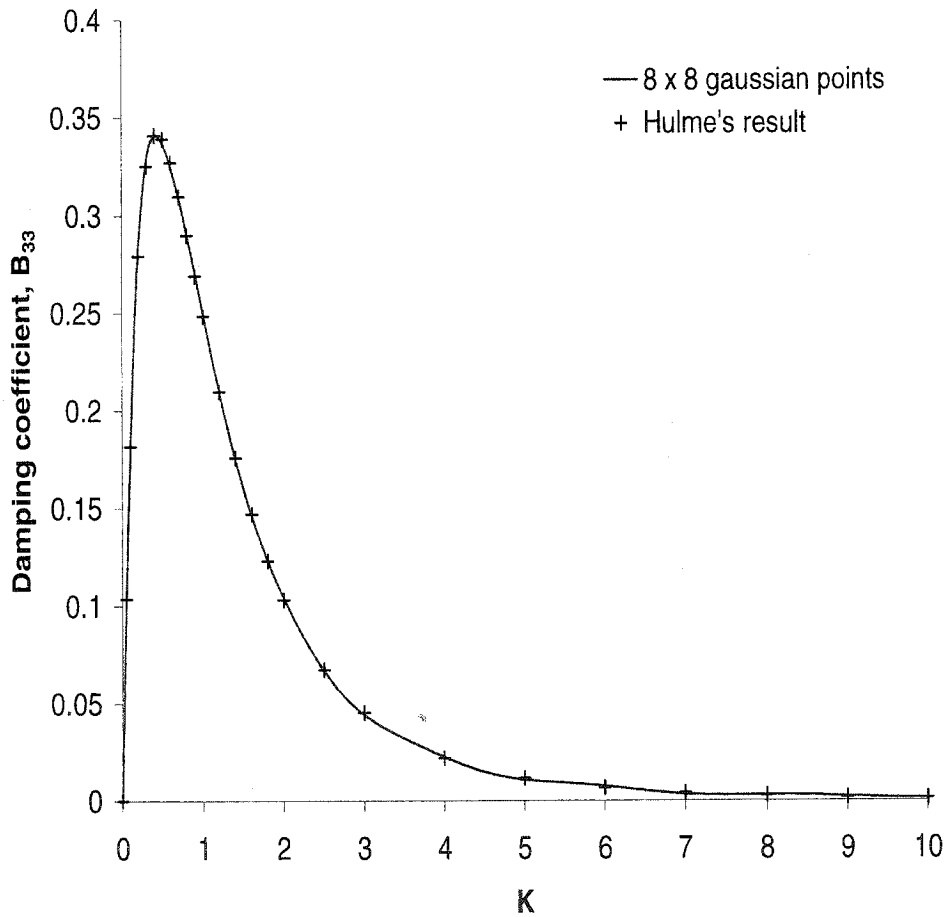

Figure 5.2: Damping coefficient in heave motion of a floating Sphere

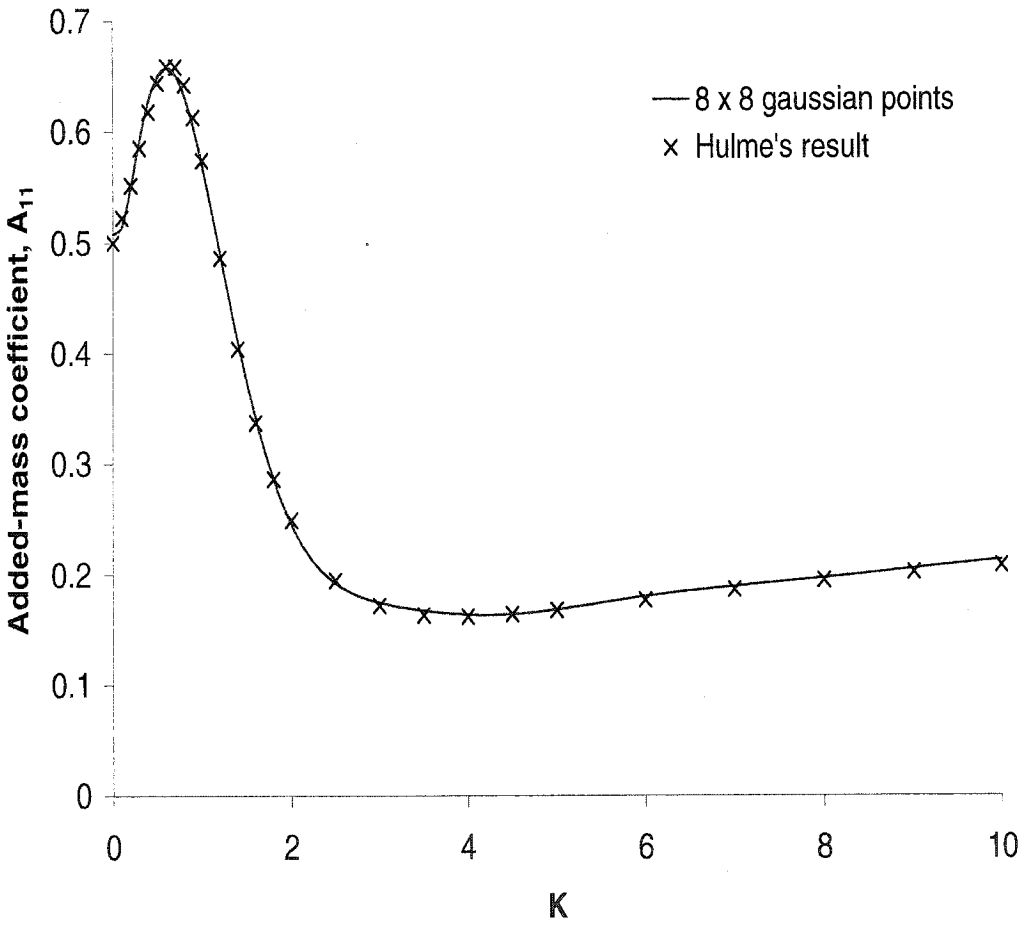

Figure 5.3: Added mass coefficient in surge motion of a floating Sphere

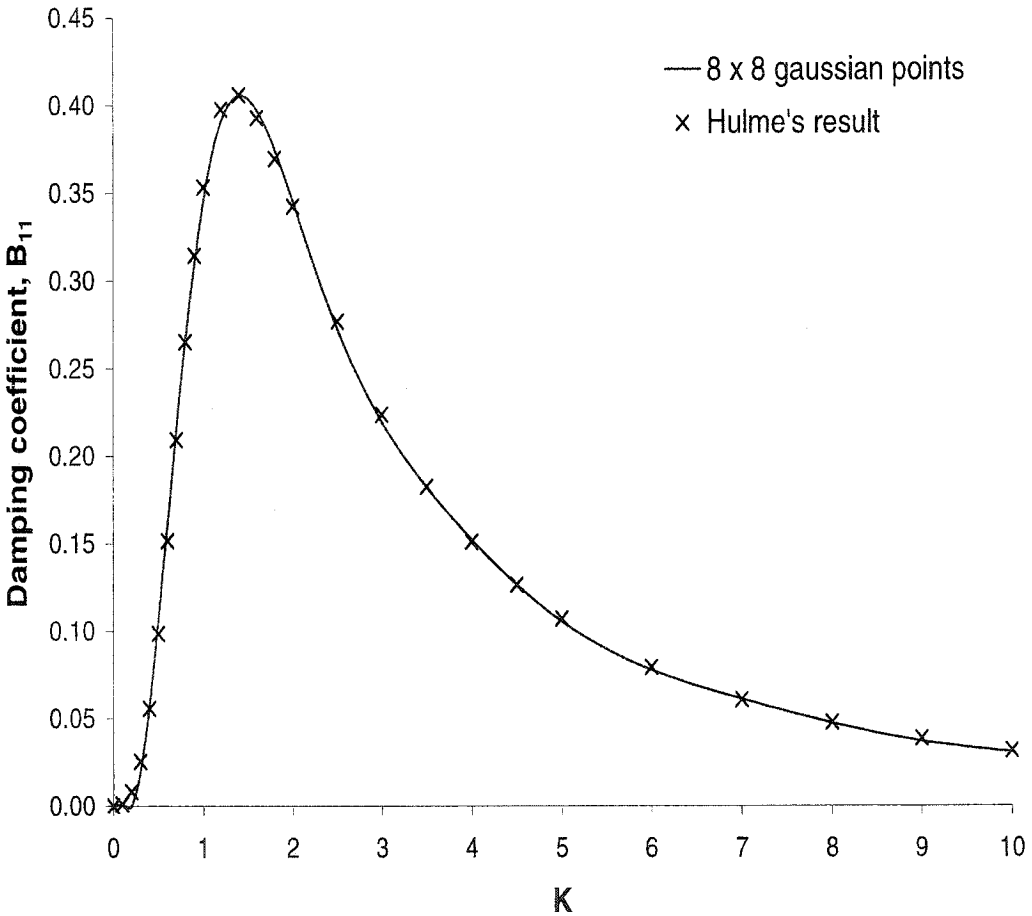

Figure 5.4: Damping coefficient in surge motion of a floating Sphere

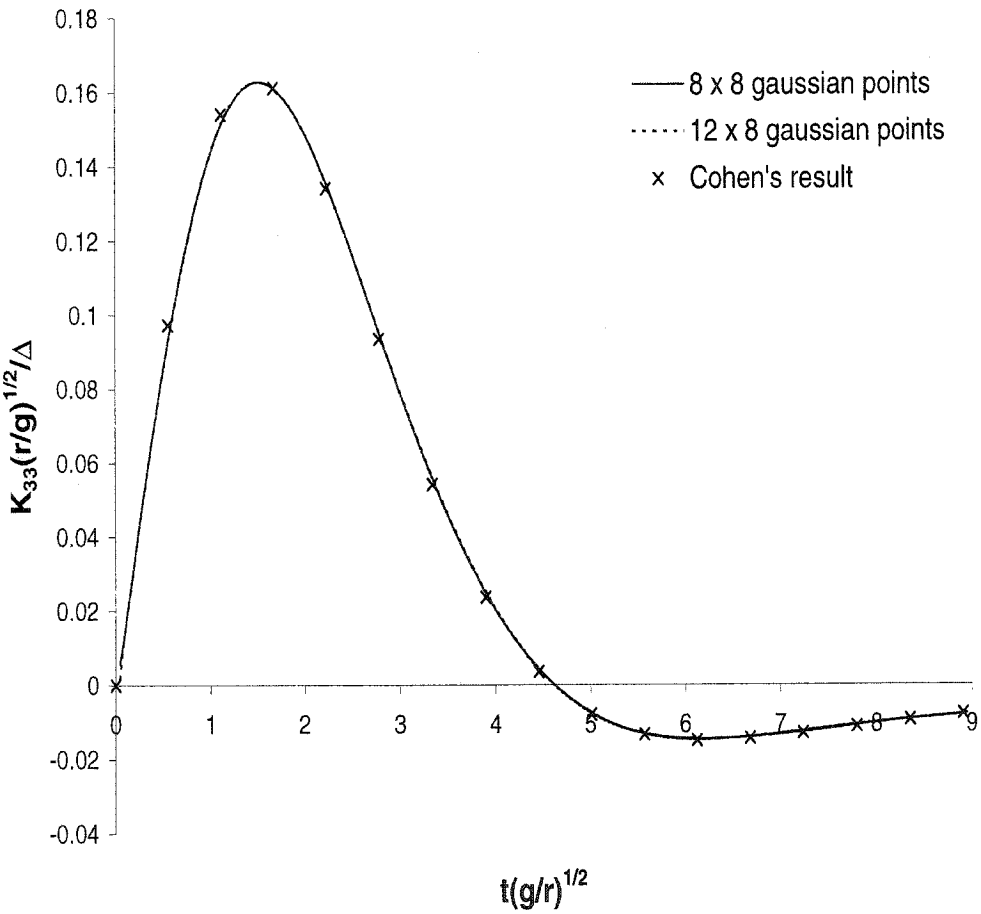

Figure 5.5: Non-dimensional heave impulsive response of a floating sphere

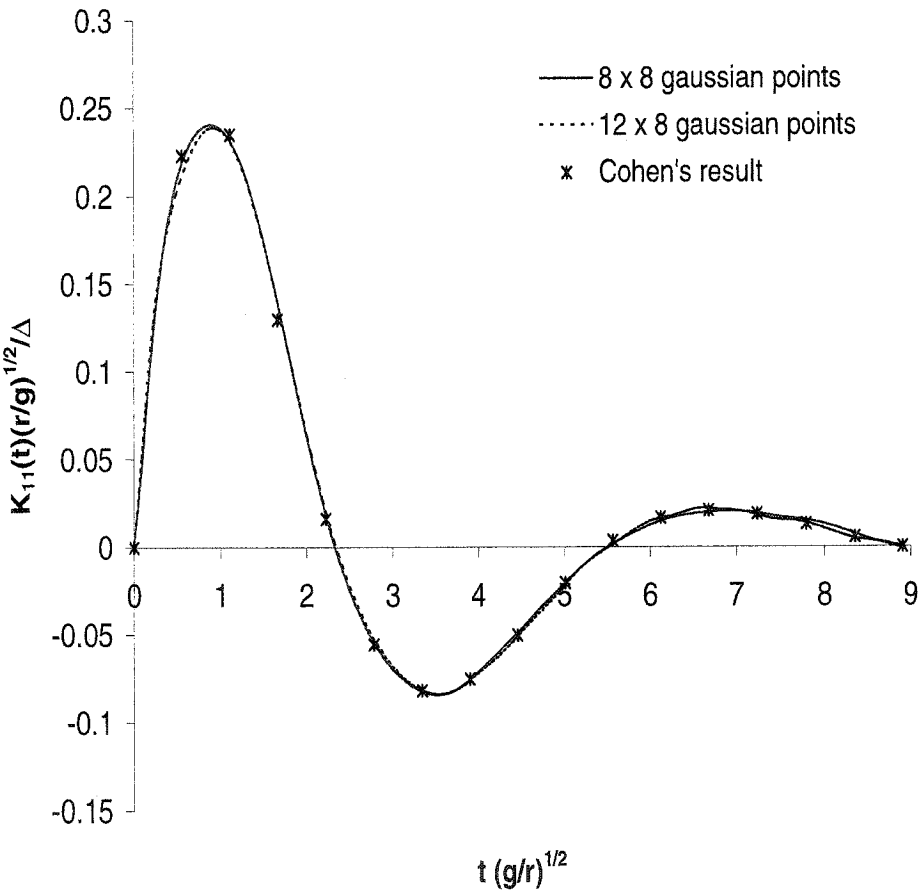

Figure 5.6: Non-dimensional surge impulsive response of a floating sphere

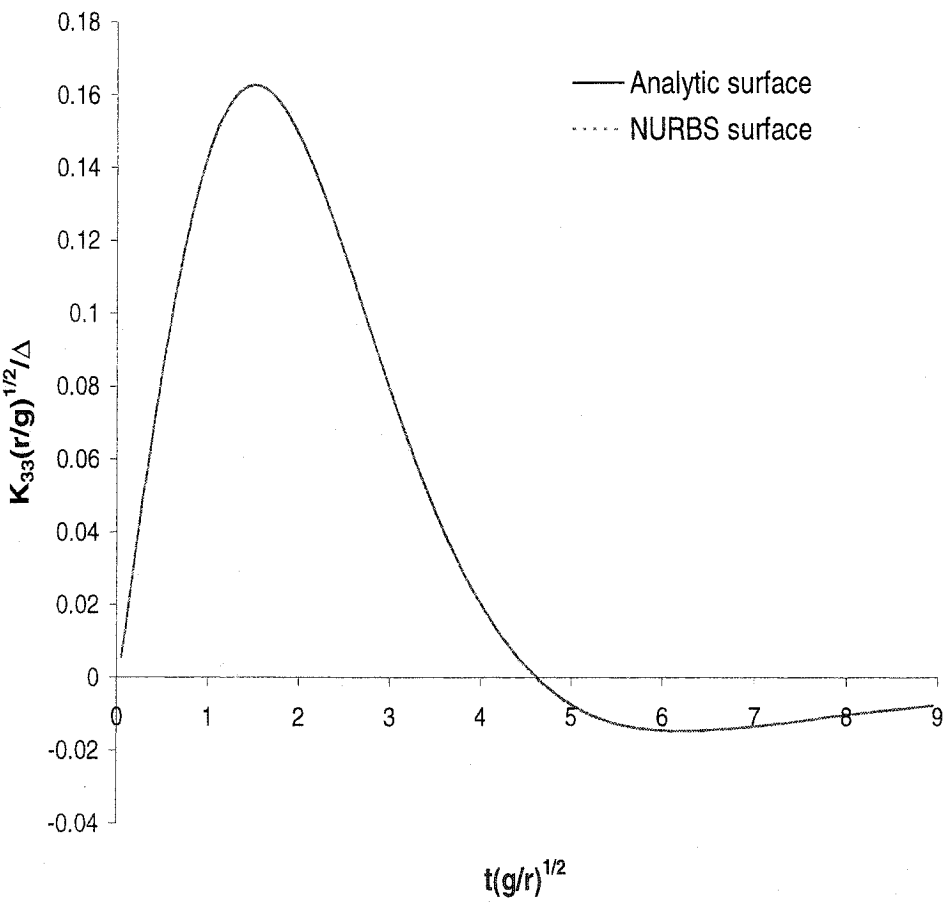

Figure 5.7: Comparison of NURBS and Analytical surfaces, 8×8 gaussian points

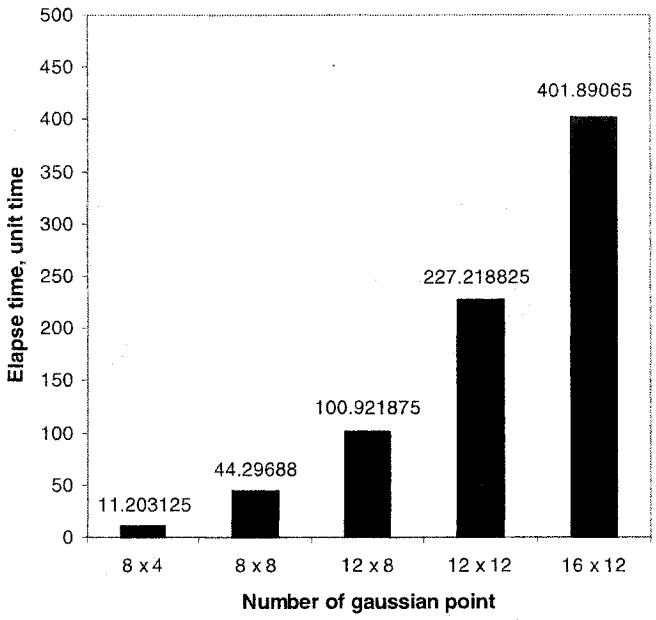

(a)

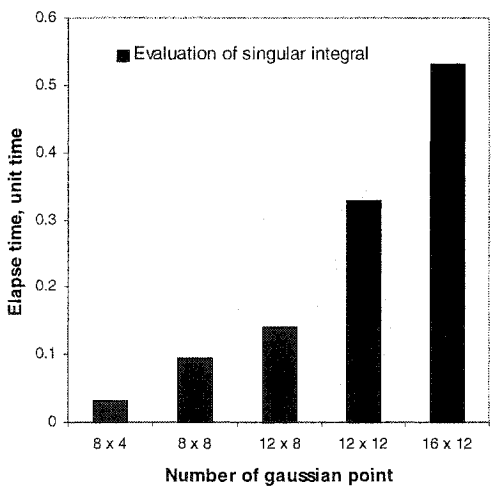

(b)

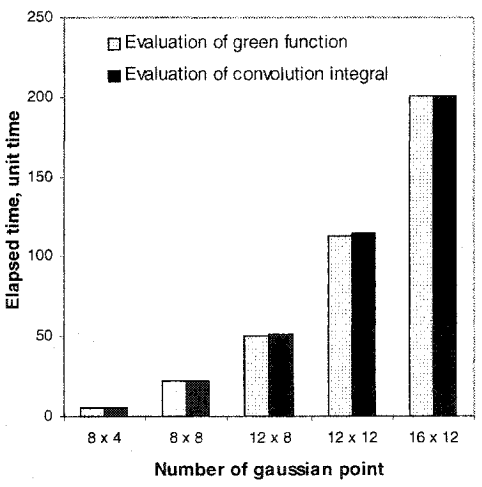

(c)

Figure 5.8: Elapsed time of $K_{33}(t)$ evaluation with $\Delta t = 0.1$

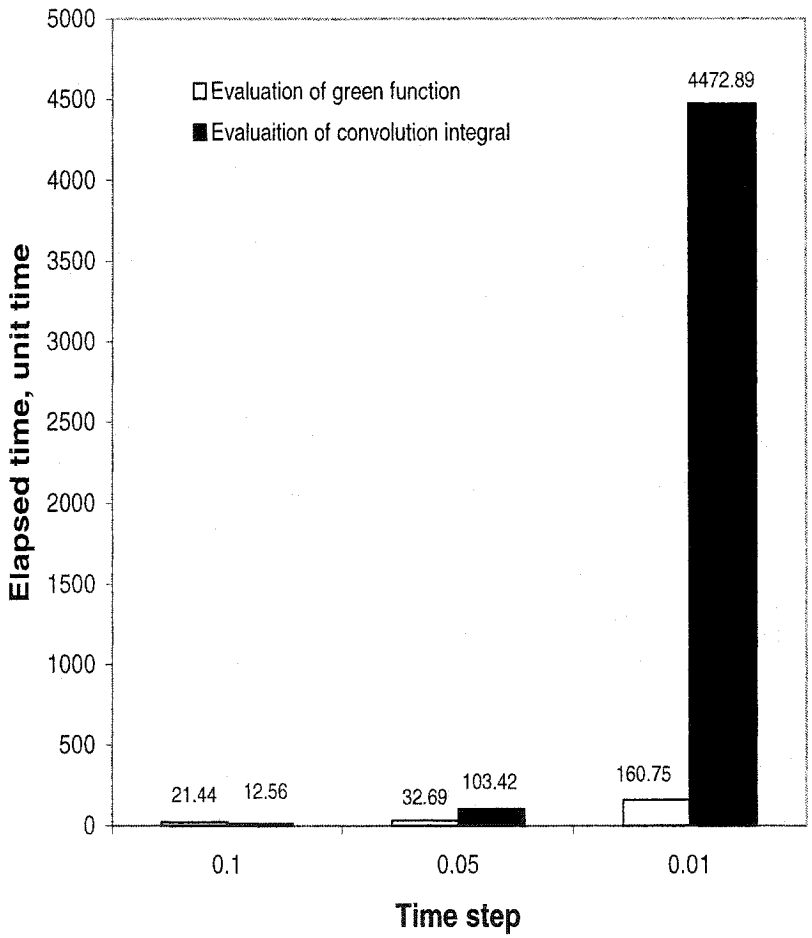

Figure 5.9: Elapsed time of $K_{33}(t)$ evaluation with $\Delta t = 0.1, 0.05$ and 0.01

Considering the discretization error, Figure 5.7 demonstrates that the same number of Gaussian points generated by the analytical surface and the NURBS surface for a floating sphere due to impulsive heave for 8×8 Gaussian points. It is shown that numerical results of the NURBS surface developed is very close to the analytical surface with a relative difference (R.D) of about 1.28E-02 where R.D is formulated as,

$$R.D = \sqrt{\frac{1}{N}\sum_{j=1}^{N}\left(\frac{K^j_{\text{analy}} - K^j_{\text{nurbs}}}{K^j_{\text{analy}}}\right)^2} \tag{5.1}$$

Yet, the error of numerical computation decreased when the number of Gaussian points increased, but unfortunetly it also influenced the time-evaluation by increasing it. Figure 5.8 presents the time-evaluation of a floating sphere due to impulsive heave, $K_{33}(t)$, for the different number of gaussiant points in which the time step of simulation is about 0.1. The time-evaluation is presented in term of elapsed time which is evaluated by subtraction of both time function set up at the first record time function with the end of the program while the codes run on PC Pentium 4, 1 Gb Mhz, 256 RAM. The total time requirement of $K_{33}(t)$ evaluation is presented in Figure 5.8 (a), and it was divided into the time-evaluation of the singularity integral, the memory part of Green's function and the convolution integral, as shown in Figures 5.8 (b) and (c), respectively. The total time-evaluation for 8×8 Gaussian points as shown in Figure 5.8 (a) increased about 200 percent when the number of Gaussian points was increased to 12×8. The relative difference (R.D) of presented in Figure 5.5 is very small, about 0.054.

Figure 5.9 shows the different time-steps, Δt, used to evaluate $K_{33}(t)$. Although the numerical error of the convolution integral decreased while the time step was decreasing, the decreasing of the time step itself increased the CPU time-consumption. The most time-consuming part of the numerical computation is the evaluation of the convolution integral at $\Delta t = 0.05$ and $\Delta t = 0.01$. The computation time at $\Delta t = 0.01$ for the convolution integral was more than 40 times that taken at $\Delta t = 0.05$. This shows the importance of optimizing the selection of Gaussian point numbers and time step, in order to achieve high accuracy without excessively increasing less CPU time-consumption.

5.2 Ellipsoid

Kim's study (1965) provides a third benchmark for the numerical results obtained by power series Green's function in evaluating of added-mass and damping coefficients of a floating ellipsoid. A half ellipsoid of length-to-beam ratio, $\bar{a}/\bar{b} = 4$ is tested evaluating the half-length-to-draft ratio, $\bar{a}/\bar{c}$ at 2and 4. The computations are performed over a range $0 \leq$ a ≤ 3.5 for the frequency parameter against added-mass as well as damping coefficients. For heaving motion, the semi-analytical result of Kim (1965) is read from the graphs for frequency parameter a, at a= $0, 0.1, 0.25, 0.5, 0.75, 1, 1.5, 2.0, 2.5, 3.0$ and 3.5.

Figure 5.10 shows the heaving added-mass coefficient as a function of the frequency parameter , a= $\bar{a}\omega^2/g$, for the ellipsoid having $\bar{a}/\bar{c} = 2$. The numerical result of an 8×8 Gaussian obtained by power series Green's function is tested against Kim's result (1965) as well as the strip method. The graph discloses good agreement between the present approach and both Kim and strip methods. The same ellipsoid is used to

obtain the damping coefficient due to impulsive heaving, and the results presented in Figure 5.11. The graph shows good agreement between the present method and Kim's and strip methods.

Figure 5.12 presents the heaving added-mass coefficient for the ellipsoid $\bar{a}/\bar{b} = 4$ as a function of frequency parameter, a. Numerical results computed using an 8×8 gaussian points were validated against Kim (1965) as well as the strip method. Figure 5.13 shows the comparison for various heaving damping coefficients. Again, the results agree reasonably well. Figure 5.10, 5.11, 5.12 and 5.13 also disclose that the values of the added-mass as well as the damping coefficient were slightly greater for ellipsoid of $\bar{a}/\bar{c} = 4$ compare to $\bar{a}/\bar{c} = 2$.

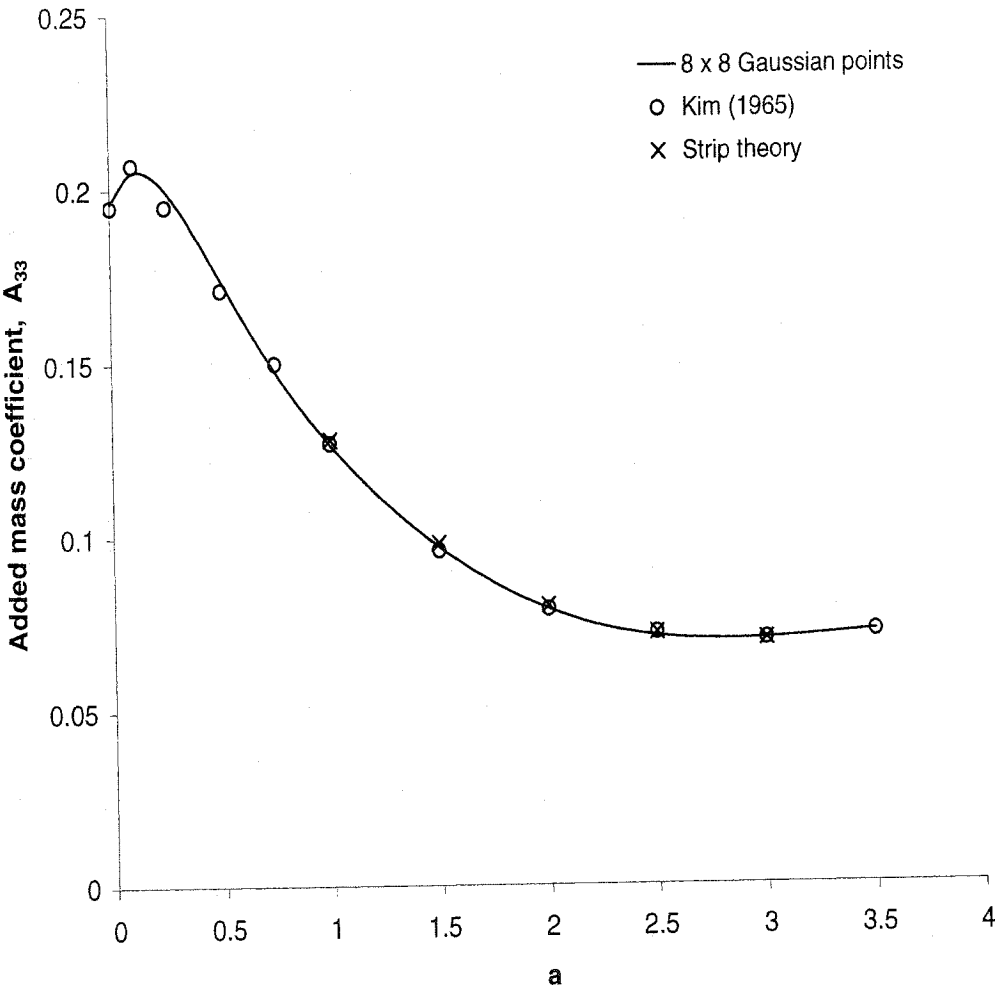

Figure 5.10: The added-mass coefficient of a floating Ellipsoid having $\bar{a}/\bar{c} = 2$, and $\bar{a}/\bar{b} = 4$ with $\bar{a} = 5$

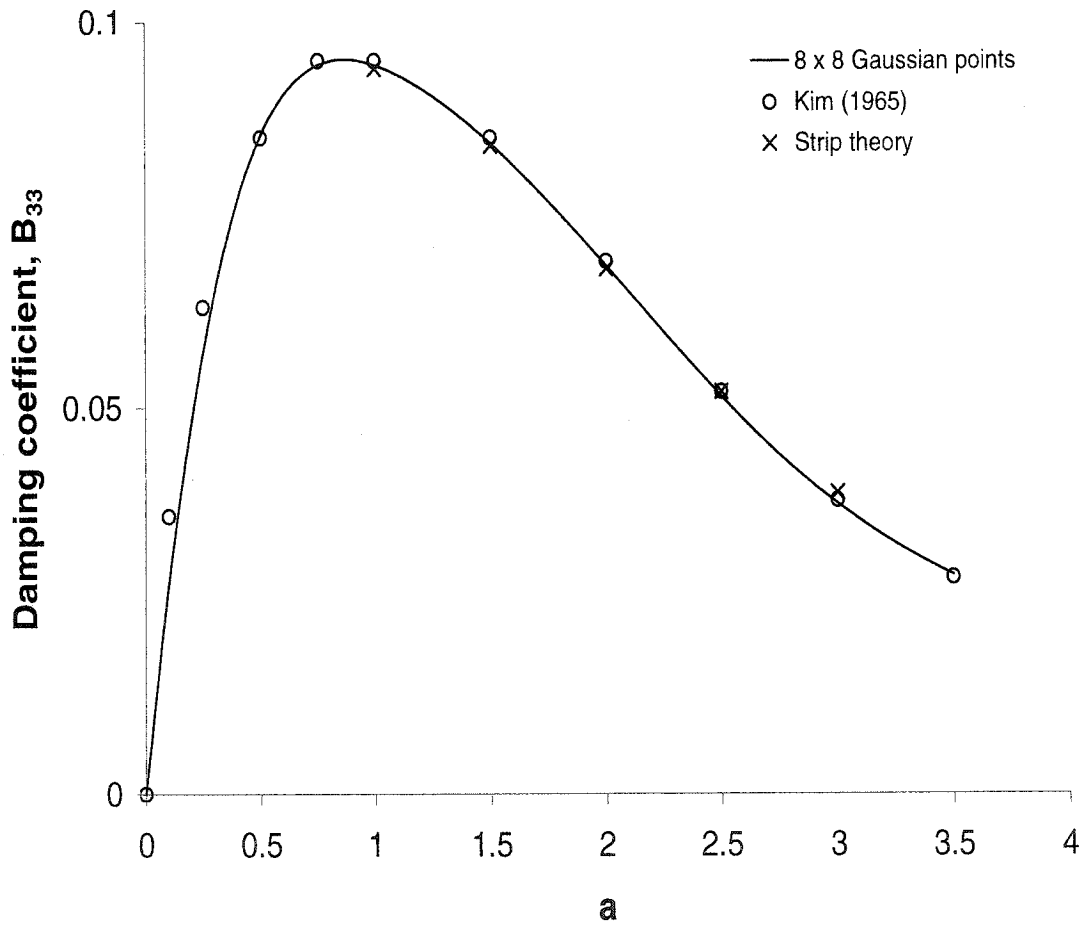

Figure 5.11: The heaving dumping coefficient of a floating Ellipsoid $\bar{a}/\bar{c} = 2$, and $\bar{a}/\bar{b} = 4$ with $\bar{a} = 5$

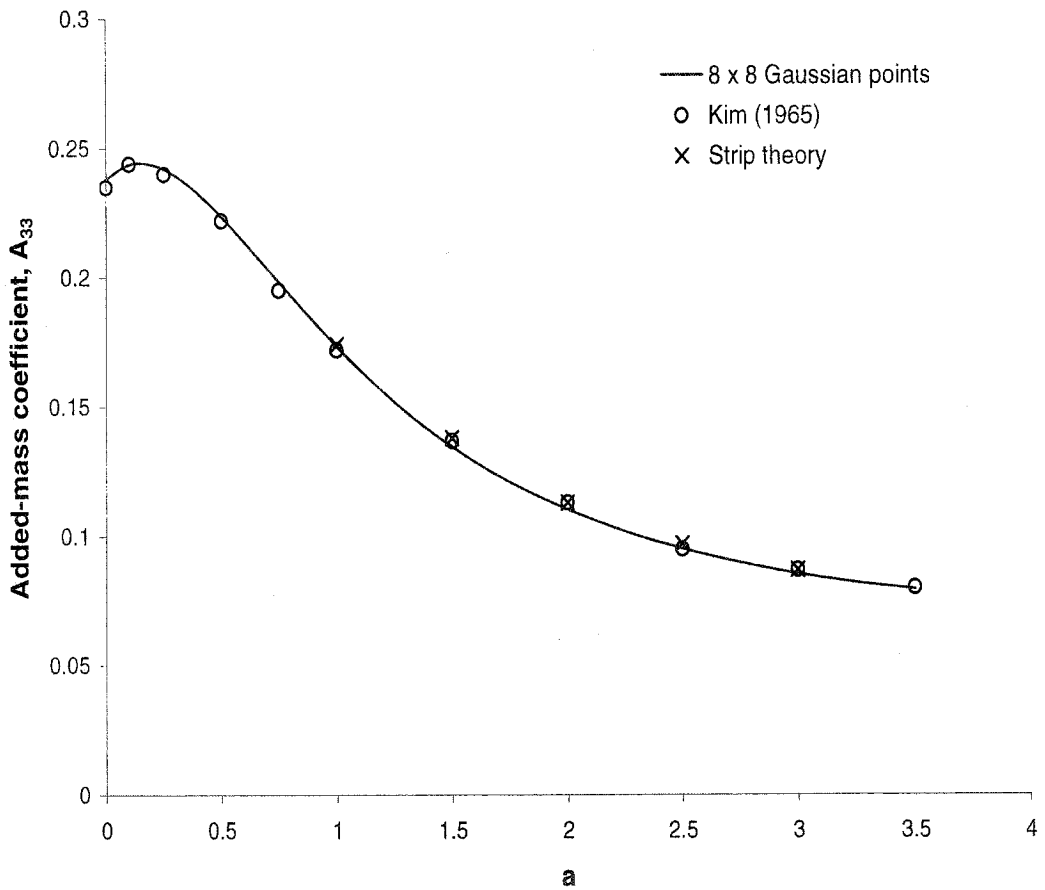

Figure 5.12: The heaving added-mass coefficient of a floating Ellipsoid $\bar{a}/\bar{c} = 4$, and $\bar{a}/\bar{b} = 4$ with $\bar{a} = 5$

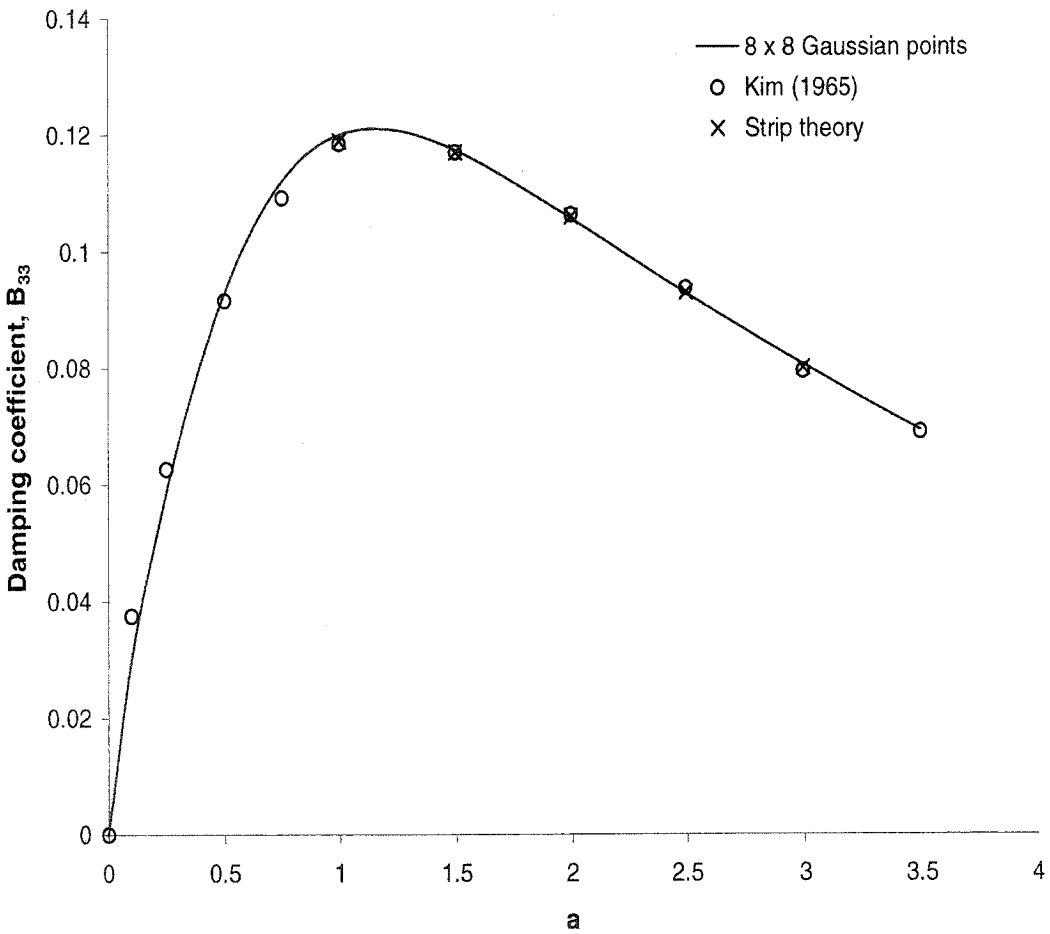

Figure 5.13: The heaving damping coefficient of a floating Ellipsoid $\bar{a}/\bar{c} = 4$, and $\bar{a}/\bar{b} = 4$ with $\bar{a} = 5$

Chapter 6

Conclusions and Recommendation

In the time-domain analysis, a major disadvantage stems from the memory effect on computation time. Because of the memory-part of Green's function and the necessity to reiterate the computation of the convolution integral at each time step, the smaller the time step, the longer the evaluation. Two techniques are proposed to reduce the CPU time. The first is to minimize time-evaluation of the memory effect of Green's function. The second is by taking off the memory-part of Green's function evaluation from the convolution integral.

The analytical procedure to evaluate the memory-part of Green's function introduced in this thesis is based on power series expansions. Numerical experiments show that the present method provides better accuracy and uses less CPU time than the fifth-order Runge-Kutta method as well as the tabulation method.

A single panel technique is introduced to evaluate the seakeeping boundary integral equation. This technique assumes the body surface as one panel, and the number of Gaussian points is generated on the surface body based on an analytical description as well as a NURBS surface. The distribution of potentials is obtained at those points. The numerical experiment showed the present technique to be more accurate

because approximation is not used in distributing potential over the body. Also, the technique is simple and is easier to formulate.

In the numerical computation, error is reduced by increasing the number of Gaussian points, but this also increases overall processing time. By reducing time-steps in the numerical simulation, errors decreased, but overall processing time steeply increased because of the time needed to compute the convolution integral. Selecting the appropriate number of Gaussian points and time-step length increase the accuracy while decreasing overall processing time. And further improvement in reducing numerical error and processing time might be addressed to the development of an alternative method for the evaluation of the convolution integrals.

Bibliography

[1] Abramowitz, M. and Stegun, I.A., Handbook of mathematical function, National bureau of standards, Washington, D.C. 1964.

[2] Adachi, H. and Ohmatsu, S. On the influence of irregular frequencies in the integral equation solutions of the time-dependent free surface problems, Journal of Engineering Mathematics, vol.16, pp.97-119, 1979

[3] Barakat, R. Vertical motion of a floating sphere in sinewave sea, Journal of Fluid Mechanics, vol.13, pp.540-556, 1962

[4] Beck, R.F. and Liapis, S.J. Transient motion of floating bodies at zero forward speed, Journal of Ship Research, vol.31, pp.167-176, 1987

[5] Beck, R.F. and Magee, A.R. Time domain analysis for predicting ship motions, Proc. of the IUTAM symmposium on dynamics of marine vehicles and structure in waves, Uxbridge, UK, 1990

[6] Bingham, H.B. Simulation ship motions in the time domain, Ph.D. Thesis, M.I.T, Massachusetts, 1994

[7] Bonnet M, Guiggiani M. Tangential derivative of singular boundary integrals with respect to the position of collocation points, International Journal for Numerical Methods in Engineering, vol.41, pp.1255-1275, 1998

[8] Clement, A.H An ordinary differential equation for Green function of time-domain free-surface hydrodynamics, Journal of Engineering Mathematics, vol.33, pp.201-217, 1998

[9] Clement, A.H Recent developments of computational time-domain hydrodynamics based on a differential approach of the Green function, Proc. Of 37th EUROTECH Colloquium, Pairiers, pp.105-114, 1998

[10] Clement, A.H. One step ahead in the numerical modeling of transient water waves: the identification of the time domain green function, Computer Modeling in Ocean Engineering, Balkema, Rotterdam, 1991

[11] Cohen, S.B. A time domain approach to three-dimensional free surface hydrodynamic interaction in narrow basins, Ph.D. Thesis, Univ. of Michigan, Ann Arbor, Michigan, 1986

[12] Cong, L.Z., Huang, Z.J., Ando, S. and Hsiung, C.C. Time-domain analysis of ship motions and hydrodynamic pressures on ship hull in waves, 2nd International Conference on Hydroelasticity in Marine Technology, Fukuoka, Japan, 1998

[13] Cummins, W.E The impulse response function and ship motion, Schiffstechnik, vol.9, pp.101-109, 1962

[14] Danmeier, D.G. A higher-order panel method for large-amplitude simulation of bodies in waves, Ph.D. Thesis, M.I.T, Massachusetts, 1999

[15] Ferrant, P. A fast computational method for transient 3D wave-body interactions, Computer Modeling in Ocean Engineering, Balkema, Rotterdam, 1988

[16] Finkelstein, A.B. The initial value problem for transient water waves, Communication on pure and applied mathematics, vol.10, pp.511-522, 1957

[17] Gradshteyn, I.S. and Ryzhik, I.M. Table of integrals, series and products, A.jeffrey (ed.), 4th edition, San Diego, Academic Press, 1965

[18] Golub, G.H. and Welsch, J.H. Calculation of Gaussian quadrature rules, Mathematics and Computation, 23, pp.221-230, 1969

[19] Hess, J. L., and Smith, A. M. O. Calculation of nonlifting potential flow about arbitrary three-dimensional bodies, Journal of Ship Research, vol.8, pp.2244, 1964.

[20] Huang, Z.J. and Hsiung, C.C A new algorithm for the three-dimensional time-domain green function, Technical report NA-91-2, Department of Mechanical Engineering, Technical University of Nova Scotia, Halifax, Nova Scotia, 1996

[21] Huang, Q and Cruse, T.A. Some notes on singular integral techniques in boundary element analysis, International Journal for Numerical Methods in Engineering, vol.36, pp.2643-2659, 1993

[22] Hulme, A. The wave forces acting on a Floating hemisphere undergoing forced periodic oscillations, Journal of Fluid Mechanics, vol.121, pp.443-463, 1982

[23] Ikebuchi, I A. Hydrodynamic forces on a body moving arbitrary in time on a free surface, Journal of Kansai Society of Naval Architecture Japan, no.181, pp.45-53, 1981

[24] Jami, A. and Pot, G. A finite-element solution for the transient flow past a freely floating body, Fourth International Conference on Numerical Ship Hydrodynamics, Washington, 1985

[25] John, F. On the motion of floating bodies II, simple harmonic motion, Communications in Pure and Applied Mathematics, vol.3, pp.45-101, 1950

[26] Kashiwagi, M., A time-domain mode-expansion method for calculating transient elastic responses of a pontoon-type VLFS, Journal of Marine Science and Technology, vol.5, pp.89-100, 2000

[27] Kim, W. D. On the harmonic oscillations of a rigid body on a free surface. Journal of Fluid Mechanics, vol.21, pp. 427-451, 1965

[28] King, B.W., Beck, R.F., and Magee, A.R. Seakeeping calculations with forward speed using time domain analysis, Proc. 17th Symposium Naval Hydrodynamics, The Hague, Netherlands, 1988

[29] King, B.W. Time domain analysis of wave exciting forces on ships and bodies, Ph.D. Thesis, Univ. of Michigan, Ann Arbor, Michigan, 1987

[30] Korsmayer, F.T. The first and second order transient free-surface wave radiation problem, Ph.D. Thesis, MIT, Cambridge, MA, 1988

[31] Lamb, H. Hydrodynamics, Dover, New York, 1932

[32] Landweber L, Macagno M. Irrotational flow about ship forms. IIHR Report No. 123, Iowa Institute of Hydraulic Research, University of Iowa, Iowa City, Iowa, 1969

[33] Lee, C.E and Sclavounos, P.D. Removing the irregular frequencies from integral equations in wave-body interaction, Journal of Fluid Mechanics, vol.207, pp.393-418, 1989

[34] Lee, C.H., Farina, L. and Newman, J.N. A geometry-independent higher-order panel method and its application to wave-body interactions, Proceeding of Engineering Mathematics and Application Conference, Adelaide, 1998

[35] Lee, C.H. and Newman, J.N. Solution of Radiation Problems with Exact Geometry, 16th International Workshop on Water Waves and Floating Bodies, Hiroshima, Japan, 2001

[36] Liapis, S.J. and Beck, R.F. Seakeeping computations using time-domain analysis, Proceedings of the fourth international symposium on numerical hydrodynamics, Washington, DC, pp.34-54, 1985

[37] Liapis, S.J. Time domain analysis of ship motion, Ph.D. Thesis, Univ. of Michigan, Ann Arbor, Michigan, 1986

[38] Lin, W.M and Yue, D.K.P. Numerical solutions for large amplitude ship motions in the time domain, Proc. 18th Symposium Naval Hydrodynamics, Ann Arbor, Michigan, 1990

[39] Magee, A.R. Large amplitude ship motions in the time domain, Ph.D. Thesis, Univ. of Michigan, Ann Arbor, Michigan, 1991

[40] Magee, A.R. and Beck, R.F. Vectorized computation of the time-domain green function, Proc. of fourth International workshop on water waves and floating bodies, Oystese, Norway, 1989

[41] Maniar, H. A three dimensional higher order panel method based on B-splines, Ph.D. thesis, MIT, Cambridge, MA, 1995

[42] Newman, J.N. Marine Hydrodynamics, MIT press, Cambridge, MA, 1977

[43] Newman, J.N. The theory of ship motions, Advances in Applied Mechanics, vol.18, pp.221-285, 1978

[44] Newman, J.N. Transient axisymmetric motion of a floating cylinder, Journal of Fluid Mechanics, vol.157, pp.17-33, 1985

[45] Newman, J.N. The evaluation of free surface Green function, Proc. 4th interl. Conference Numerical Ship Hydrodynamics, Washington DC, 1985

[46] Newman, J.N. The approximation of free-surface Green function,

[47] Ogilvie, T.F. Recent progress toward the understanding and prediction of ship motions. Procedings 5th Symposium on Naval Hydrodynamics, Washington, D.C., pp. 3-128, 1964

[48] Ohmatsu, S. On the irregular frequencies in the theory of oscillating bodies in a free surface. Papers Ship Res. Inst. Japan, No. 48, 1975

[49] Pot, G and Jami, A. Some numerical results in 3-D transient linear naval hydrodynamics, Journal of Ship Research, vol.35, no.4, pp.295-303, 1991

[50] Piegl, L. and Tiller, W. The NURBS book, Springer, New York, 1997

[51] Qiu, W. A panel-free method for time-domain analysis of floating bodies in waves, Ph.D Thesis, Dalhousie University, Halifax, 2001

[52] Rahman, M. Applied differential equations for scientist and engineers: Ordinary Differential Equations, Computational Mechanics Publications, 1991

[53] Sheng, J. Ship geometry approximation using non-uniform rational B-splines with application to computational hydrodynamics, Master Thesis, Dalhousie University, Halifax, 2002

[54] Sladek, V. and Sladek, J. Singular Integrals in Boundary Element Methods, Computational Mechanics Publications, Southampton, 1998

[55] Spiegel, M.R. Mathematical handbook of formulas and tables, Schaum's outline series, Mcgraw-hill, 1968

[56] Sulisetyono, A, and Islam, M.R. Analytic solution of the memory part of the time domain green function, International mathematical journal, vol.6, no.1, 2005

[57] Tanaka, M., Sladek, V., and Sladek, J. Regularization techniques applied to boundary element methods, Applied Mechanics Reviews, vol.47, pp.457-499, 1994

[58] Wehausen, J.V., and Laitone, E.V. Surface waves, Handbuch der physic, Springer-Verlag, Berlin, pp. 446-778, 1960

[59] Wehausen, J.V. The motion of floating bodies, Annual Review of Fluid Mechanics, vol.3, pp.237-268, 1971

[60] Wylie, C. and Barret, L. Advanced engineering mathematics, Mcgraw-hill, 1961

[61] Yang, S.A. On the singularities of Green's formula and its normal derivative, with an application to surface-wave-body interaction problems, Int. J. Numer. Meth. Engng., vol.47, pp.1841-1864, 2000

[62] Yeung, R.W. The transient heaving motion of floating cylinder, Journal of Engineering Mathematics, vol.16, pp.97-119, 1982

[63] Zhang, S. and Jin, J. Computation of special functions, John Wiley, New York, 1996

Appendix A

Boundary Integral Equation over Free-Surface and Infinity Bounding Surface

A.1 The integral over free surface, S_F

Considering the integral over the free surface, let write boundary integral equation as,

$$\begin{aligned} I_{S_F} &= \int_0^t d\tau \int_{S_F(\tau)} \Big\{ \phi(Q,\tau) \frac{\partial G}{\partial n_Q}(P,Q;t-\tau) \\ &- \frac{\partial \phi}{\partial n_Q}(Q,\tau) G(P,Q;t-\tau) \Big\} dS_Q \end{aligned} \tag{A.1}$$

On the free surface, both the velocity potential, ϕ, and the Green's function, G, satisfy the linearized free suraface condition such as,

$$\frac{\partial \phi}{\partial n_Q}(Q,\tau) = -\frac{\partial^2 \phi}{\partial \tau^2}(Q,\tau), \qquad \frac{\partial G}{\partial n_Q}(P,Q;t-\tau) = -\frac{\partial^2 G}{\partial \tau^2}(P,Q;t-\tau) \tag{A.2}$$

Substituting Eqn (A.2) into Eqn (A.1), the integral over the free surface becomes:

$$\begin{aligned} I_{S_F} &= -\int_0^t d\tau \int_{S_F(\tau)} \Big\{ \phi(Q,\tau) \frac{\partial^2 G}{\partial^2 \tau}(P,Q;t-\tau) \\ &\quad -\frac{\partial^2 \phi}{\partial^2 \tau}(Q,\tau) G(P,Q;t-\tau) \Big\} dS_Q \end{aligned} \tag{A.3}$$

It can be rearrangement as,

$$\begin{aligned} I_{S_F} &= -\int_0^t d\tau \int_{S_F(\tau)} \frac{\partial}{\partial \tau} \Big\{ \phi(Q,\tau) \frac{\partial G}{\partial \tau}(P,Q;t-\tau) \\ &\quad -\frac{\partial \phi}{\partial \tau}(Q,\tau) G(P,Q;t-\tau) \Big\} dS_Q \end{aligned} \tag{A.4}$$

Let introduce the transport theorem which can be applied for two-dimensional domain such as:

$$\frac{d}{d\tau} \int_{S_F(\tau)} dS_Q f(Q,\tau) = \int_{S_F(\tau)} dS_Q \frac{\partial}{\partial \tau} f(Q,\tau) + \oint_L (\tau) dl_Q V_n f(Q,\tau) \tag{A.5}$$

and let take

$$f(Q,\tau) = \left\{\phi(Q,\tau)\frac{\partial G}{\partial \tau}(P,Q;t-\tau) - \frac{\partial \phi}{\partial \tau}(Q,\tau)G(P,Q;t-\tau)\right\} \tag{A.6}$$

Substitute Eqn (A.6) into Eqn (A.5), the total derivative in τ of the integral over S_F can be written as,

$$\begin{aligned}
&\int_{S_F(\tau)} \frac{\partial}{\partial \tau}\Big[\phi(Q,\tau)\frac{\partial G}{\partial \tau}(P,Q;t-\tau) - G(P,Q;t-\tau)\frac{\partial \phi}{\partial \tau}(Q,\tau)\Big]dS_Q \\
&= \frac{d}{d\tau}\int_{S_F(\tau)} \Big[\phi(Q,\tau)\frac{\partial G}{\partial \tau}(P,Q;t-\tau) - G(P,Q;t-\tau)\frac{\partial \phi}{\partial \tau}(Q,\tau)\Big]dS_Q \\
&- \oint_{S_L(\tau)} \Big[\phi(Q,\tau)\frac{\partial G}{\partial \tau}(P,Q;t-\tau) - G(P,Q;t-\tau)\frac{\partial \phi}{\partial \tau}(Q,\tau)\Big]V_n dl_Q
\end{aligned} \tag{A.7}$$

where L is the curve defined by the intersection of the instantaneous body surface S_B on the free surface, $z = 0$, and V_n is the two-dimensional normal velocity of a point on L. The line integral which is last term of Eqn (A.7) obviously vanished, when the body is fully submerged as well as when L is time invariant which is the linear problem without forward speed. Consider to both cases the floating body and submerged body with zero speed, Eqn(A.7) is substited into Eqn (A.4) with vanished line integral, we may written for I_{S_F} as,

$$\begin{aligned}
I_{S_F} \;=\; & -\int_0^t d\tau \frac{d}{d\tau}\int_{S_F(\tau)} \Big\{\phi(Q,\tau)\frac{\partial G}{\partial \tau}(P,Q;t-\tau) \\
& -\frac{\partial \phi}{\partial \tau}(Q,\tau)G(P,Q;t-\tau)\Big\}dS_Q
\end{aligned} \tag{A.8}$$

Due to the initial condition for $\frac{\partial G}{\partial \tau} = 0$ and $\frac{\partial \phi}{\partial \tau} = 0$, so this term is zero.

A.2 The integral over infinity bounding surface, S_∞

We next consider the integral over bounding surface at infinity, let write boundary integral equation as,

$$\begin{aligned} I_{S_\infty} &= \int_0^t d\tau \int_{S_\infty(\tau)} \Big\{ \phi(Q,\tau) \frac{\partial G}{\partial n_Q}(P,Q;t-\tau) \\ &\quad - \frac{\partial \phi}{\partial n_Q}(Q,\tau) G(P,Q;t-\tau) \Big\} dS_Q \end{aligned} \tag{A.9}$$

Since the potential, ϕ and the Green's function, G, both being bounded at infinity condition, the integral over infinity bounding surface in Eqn (A.9) is equal to zero due to the Infinity condition.

Appendix B

Derivation of the nine terms fourth order ordinary differential equation of the free-surface Green's function

Clément's approach (1998a) introduced the procedure to derive Eqn (3.3) to be the fourth order ordinary differential equation. Based on his procedure we expanded into the nine terms fourth order differential equation in which the power series expansion can be applied. Let us take Eqn (3.3) with the second and fourth derivatives.

$$F_1(\mu,\beta) = \int_0^\infty J_0(\sqrt{(1-\mu^2)}\lambda)e^{-\lambda\mu}\sqrt{\lambda}\sin(\beta\sqrt{\lambda})d\lambda \tag{B.1}$$

$$-\frac{d^2F_1}{d\beta^2}(\mu,\beta) = \int_0^\infty J_0(\lambda\sqrt{1-\mu^2})e^{-\lambda\mu}\lambda^{3/2}\sin(\sqrt{\lambda}\beta]d\lambda \tag{B.2}$$

$$\frac{d^4F_1}{d\beta^4}(\mu,\beta) = \int_0^\infty J_0(\lambda\sqrt{1-\mu^2})e^{-\lambda\mu}\lambda^{5/2}\sin(\sqrt{\lambda}\beta]d\lambda \tag{B.3}$$

Introduce new variables, $\lambda = q/\beta^2$ and $d\lambda = dq/\beta^2$, and substitute into Eqn (B.1), (B.2) and (B.3) respectively as:

$$F_1(\mu,\beta) = \frac{1}{\beta^3}\int_0^\infty J_0\Big(\frac{q\sqrt{1-\mu^2}}{\beta}\Big)e^{-\frac{q\mu}{\beta^2}}q^{1/2}\sin(\sqrt{q})dq \tag{B.4}$$

$$-\frac{d^2F_1}{d\beta^2}(\mu,\beta) = \frac{1}{\beta^5}\int_0^\infty J_0\Big(\frac{q\sqrt{1-\mu^2}}{\beta}\Big)e^{-\frac{q\mu}{\beta^2}}q^{3/2}\sin(\sqrt{q})dq \tag{B.5}$$

$$\frac{d^4F_1}{d\beta^4}(\mu,\beta) = \frac{1}{\beta^7}\int_0^\infty J_0\Big(\frac{q\sqrt{1-\mu^2}}{\beta}\Big)e^{-\frac{q\mu}{\beta^2}}q^{5/2}\sin(\sqrt{q})dq \tag{B.6}$$

Introduce another new variable, $\beta^2 = 1/v$ and $\beta = \sqrt{1/v}$, and substitute into Eqn (B.4), (B.5) and (B.6) respectively to yield:

$$F_1(\mu,v) = \int_0^\infty J_0\Big(vq\sqrt{1-\mu^2}\Big)v^{3/2}e^{-vq\mu}q^{1/2}\sin(\sqrt{q})dq \tag{B.7}$$

$$-\beta^2\frac{d^2F_1}{d\beta^2}(\mu,v) = \int_0^\infty J_0\Big(vq\sqrt{1-\mu^2}\Big)v^{3/2}e^{-vq\mu}q^{3/2}\sin(\sqrt{q})dq \tag{B.8}$$

$$\beta^4\frac{d^4F_1}{\beta^4}(\mu,v) = \int_0^\infty J_0\Big(vq\sqrt{1-\mu^2}\Big)v^{3/2}e^{-vq\mu}q^{5/2}\sin(\sqrt{q})dq \tag{B.9}$$

The Bessel function $J_0(\Big(vq\sqrt{1-\mu^2}\Big)$ can be expressed in term of the Hypergeometric Function as [see Abramowitz and Stegun(1964), Eqn 9.1.69]

$$J_0\Big(vq\sqrt{1-\mu^2}\Big) = e^{-jvq\sqrt{1-\mu^2}}M\Big(\frac{1}{2},1,2jvq\sqrt{1-\mu^2}\Big) \tag{B.10}$$

Substitute Eqn (B.10) into Eqn (B.7), (B.8) and (B.9) respectively, yields

$$F_1(\mu, v) = \int_0^\infty W(q, v, \mu) q^{1/2} \sin(\sqrt{q}) dq \tag{B.11}$$

$$-\beta^2 \frac{d^2 F_1}{d\beta^2}(\mu, v) = \int_0^\infty W(q, v, \mu) q^{3/2} \sin(\sqrt{q}) dq \tag{B.12}$$

$$\beta^4 \frac{d^4 F_1}{\beta^4}(\mu, v) = \int_0^\infty W(q, v, \mu) q^{5/2} \sin(\sqrt{q}) dq \tag{B.13}$$

where

$$W(q, v, \mu) = v^{3/2} e^{-vq(\mu + j\sqrt{1-\mu^2})} M\Big(\frac{1}{2}, 1, 2jvq\sqrt{1-\mu^2}\Big) \tag{B.14}$$

Eqn (B.14) can be simplified as,

$$W(q, v, \mu) = v^{-A} e^{-f(v)} M\Big(a, b, g(v)\Big) \tag{B.15}$$

where,

$$\begin{aligned} A &= -\frac{3}{2}; \quad a = \frac{1}{2}; \quad b = 1 \\ f(v) &= vq(\mu + j\sqrt{1-\mu^2}); \quad \frac{df}{dv}(v) = q(\mu + j\sqrt{1-\mu^2}) \\ g(v) &= 2jvq\sqrt{1-\mu^2}; \quad \frac{dg}{dv}(v) = 2jq\sqrt{1-\mu^2} \end{aligned} \tag{B.16}$$

Expression of Eqn (B.15) is the solution of Eqn (B.17) which is the general confluent equation [see Abramowitz and Stegun(1964), Eqn. 13.1.35]

$$\frac{d^2W}{dv^2} + \Big\{\frac{2A}{v} + 2\frac{df}{dv}(v) + \frac{b}{g(v)}\frac{dg}{dv}(v) - \frac{dg}{dv}(v) - \frac{d^2g/dv^2(v)}{dg/dv(v)}\Big\}\frac{dW}{dv}$$
$$+\Big\{\Big(\frac{b}{g(v)}\frac{dg}{dv}(v) - \frac{dg}{dv}(v) - \frac{d^2g/dv^2(v)}{dg/dv(v)}\Big)\Big(\frac{A}{v} + \frac{df}{dv}(v)\Big) + \frac{A(A-1)}{v^2}$$
$$+\frac{2A}{v}\frac{df}{dv} + \frac{d^2f}{dv^2} + \Big(\frac{df}{dv}\Big)^2 - \frac{a}{g(v)}\Big(\frac{dg}{dv}\Big)^2\Big\} = 0 \qquad \text{(B.17)}$$

Substituting Eqn (B.16) into Eqn (B.17) yields,

$$\frac{d^2W}{dv^2} - 2\Big(\frac{1}{v} - q\mu\Big)\frac{dW}{dv} + \Big(q^2 - \frac{4q\mu}{v} + \frac{9}{4v^2}\Big)W = 0 \qquad \text{(B.18)}$$

Therefore let

$$\begin{aligned} v &= \frac{1}{\beta^2} \\ \frac{d}{dv} &= -\frac{1}{2}\beta^3\frac{d}{d\beta} \\ \frac{d^2}{dv^2} &= \frac{3}{4}\beta^5\frac{d}{d\beta} + \frac{1}{4}\beta^6\frac{d^2}{d\beta^2} \end{aligned} \qquad \text{(B.19)}$$

Substituting Eqn (B.19) into Eqn (B.18), yields:

$$\frac{1}{4}\beta^6\frac{d^2W}{d\beta^2}+\Big(\frac{7}{4}\beta^5-\mu q\beta^3\Big)\frac{dW}{d\beta}+\Big(q^2-4\mu q\beta^2+\frac{9}{4}\beta^4\Big)W=0 \tag{B.20}$$

Rearranging Eqn (B.20), by moving the term with variable q to the right hand side, yields:

$$\frac{1}{4}\beta^6\frac{d^2W}{d\beta^2}+\frac{7}{4}\beta^5\frac{dW}{d\beta}+\frac{9}{4}\beta^4W=\mu q\beta^3\frac{dW}{d\beta}-\Big(q^2-4\mu q\beta^2\Big)W \tag{B.21}$$

Eqn (B.21) is divided by β^4. Introduce β_1 as constant, and by 'add and substract' technique Eqn (B.21) can be rearranged into ten terms as:

$$\begin{aligned}&\frac{1}{4}(\beta-\beta_1)^2\frac{d^2W}{d\beta^2}+\frac{1}{2}\beta_1(\beta-\beta_1)\frac{d^2W}{d\beta^2}+\frac{1}{4}\beta_1^2\frac{d^2W}{d\beta^2}+\frac{7}{4}(\beta-\beta_1)\frac{dW}{d\beta}\\&+\frac{7}{4}\beta_1\frac{dW}{d\beta}+\frac{9}{4}W=\frac{\mu q(\beta-\beta_1)}{\beta^2}\frac{dW}{d\beta}+\frac{\mu q\beta_1}{\beta^2}\frac{dW}{d\beta}-\frac{q^2}{\beta^4}W+\frac{4\mu q}{\beta^2}W\end{aligned} \tag{B.22}$$

Multiply both left and right hand sides of Eqn (B.22) by $q^{1/2}\sin(\sqrt{q})$ and integrate with respect to q, from 0 to ∞.

$$\begin{aligned}&\frac{1}{4}(\beta-\beta_1)^2\frac{d^2}{d\beta^2}\Big(\int_0^\infty W(q,v,\mu)q^{1/2}\sin(\sqrt{q})dq\Big)\\&+\frac{1}{2}\beta_1(\beta-\beta_1)\frac{d^2}{d\beta}\Big(\int_0^\infty W(q,v,\mu)q^{1/2}\sin(\sqrt{q})dq\Big)\\&+\frac{1}{4}\beta_1^2\frac{d^2}{d\beta^2}\Big(\int_0^\infty W(q,v,\mu)q^{1/2}\sin(\sqrt{q})dq\Big)\\&+\frac{7}{4}(\beta-\beta_1)\frac{d}{d\beta}\int_0^\infty W(q,v,\mu)q^{1/2}\sin(\sqrt{q})dq\end{aligned}$$

$$
\begin{aligned}
&+\frac{7}{4}\beta_1\frac{d}{d\beta}\Big(\int_0^\infty W(q,v,\mu)q^{1/2}\sin(\sqrt{q})dq\Big)\\
&+\frac{9}{4}\Big(\int_0^\infty W(q,v,\mu)q^{1/2}\sin(\sqrt{q})dq\Big)\\
&=\frac{\mu(\beta-\beta_1)}{\beta^2}\frac{d}{d\beta}\Big(\int_0^\infty W(q,v,\mu)q^{3/2}\sin(\sqrt{q})dq\Big)\\
&+\frac{\mu\beta_1}{\beta^2}\frac{d}{d\beta}\Big(\int_0^\infty W(q,v,\mu)q^{3/2}\sin(\sqrt{q})dq\Big)\\
&-\frac{1}{\beta^4}\Big(\int_0^\infty W(q,v,\mu)q^{5/2}\sin(\sqrt{q})dq\Big)\\
&+\frac{4\mu}{\beta^2}\Big(\int_0^\infty W(q,v,\mu)q^{3/2}\sin(\sqrt{q})dq\Big)
\end{aligned}
\tag{B.23}
$$

Substituting Eqn (B.11), (B.12) and (B.13) into Eqn (B.23), yields

$$
\begin{aligned}
&\frac{1}{4}(\beta-\beta_1)^2\frac{d^2F_1}{d\beta^2}+\frac{1}{2}\beta_1(\beta-\beta_1)\frac{d^2F_1}{d\beta^2}+\frac{1}{4}\beta_1^2\frac{d^2F_1}{d\beta^2}+\frac{7}{4}(\beta-\beta_1)\frac{dF_1}{d\beta}\\
&+\frac{7}{4}\beta_1\frac{dF_1}{d\beta}+\frac{9}{4}F_1=\frac{\mu(\beta-\beta_1)}{\beta^2}\frac{d}{d\beta}\Big(-\beta^2\frac{d^2F_1}{d\beta^2}\Big)+\frac{\mu\beta_1}{\beta^2}\frac{d}{d\beta}\Big(-\beta^2\frac{d^2F_1}{d\beta^2}\Big)\\
&-\frac{1}{\beta^4}\Big(\beta^4\frac{d^4F_1}{\beta^4}\Big)+\frac{4\mu}{\beta^2}\Big(-\beta^2\frac{d^2F_1}{d\beta^2}\Big)
\end{aligned}
\tag{B.24}
$$

Simplifying Eqn (B.24) into nine terms, this becomes:

$$
\begin{aligned}
&\frac{d^4F_1}{d\beta^4}+\mu(\beta-\beta_1)\frac{d^3F_1}{d\beta^3}+\mu\beta_1\frac{d^3F_1}{d\beta^3}+\frac{1}{4}(\beta-\beta_1)^2\frac{d^2F_1}{d\beta^2}\\
&+\frac{1}{2}\beta_1(\beta-\beta_1)\frac{d^2F_1}{d\beta^2}+\Big(\frac{1}{4}\beta_1^2+4\mu\Big)\frac{d^2F_1}{d\beta^2}\\
&+\frac{7}{4}(\beta-\beta_1)\frac{dF_1}{d\beta}+\frac{7}{4}\beta_1\frac{dF_1}{d\beta}+\frac{9}{4}F_1=0
\end{aligned}
\tag{B.25}
$$

For the sake of simplicity, let us define

$$x_1 = 1;\ x_2 = \mu;\ x_3 = \mu\beta_1;\ x_4 = \frac{1}{4};\ x_5 = \frac{1}{2}\beta_1;$$
$$x_6 = \frac{1}{4}\beta_1^2 + 4\mu;\ x_7 = \frac{7}{4};\ x_8 = \frac{7}{4}\beta_1;\ x_9 = \frac{9}{4} \tag{B.26}$$

Therefore substituting Eqn (B.26) into Eqn (B.25):

$$x_1\frac{d^4F_1}{d\beta^4} + x_2(\beta-\beta_1)\frac{d^3F_1}{d\beta^3} + x_3\frac{d^3F_1}{d\beta^3} + x_4(\beta-\beta_1)^2\frac{d^2F_1}{d\beta^2}$$
$$+x_5(\beta-\beta_1)\frac{d^2F_1}{d\beta^2} + x_6\frac{d^2F_1}{d\beta^2} + x_7(\beta-\beta_1)\frac{dF_1}{d\beta}(\beta)$$
$$+x_8\frac{dF_1}{d\beta} + x_9F_1 = 0 \tag{B.27}$$

Following the previous step, the solution of $F_2(\mu,\beta)$ and $F_3(\mu,\beta)$ functions in Eqn (3.8) and Eqn (3.9) repectively can also be expanded into nine terms similar to Eqn (B.27). The different nine variable coefficients of $F_2(\mu,\beta)$ and $F_3(\mu,\beta)$ functions can be defined respectively as:

$$y_1 = 1;\ y_2 = \mu;\ y_3 = \mu\beta_1;\ y_4 = \frac{1}{4};\ y_5 = \frac{1}{2}\beta_1;$$
$$y_6 = \frac{1}{4}\beta_1^2 + 4\mu;\ y_7 = \frac{11}{4};\ y_8 = \frac{11}{4}\beta_1;\ y_9 = \frac{21}{4} \tag{B.28}$$

and

$$z_1 = 1;\ z_2 = \mu;\ z_3 = \mu\beta_1;\ z_4 = \frac{1}{4};\ z_5 = \frac{1}{2}\beta_1;$$
$$z_6 = \frac{1}{4}\beta_1^2 + 4\mu;\ z_7 = \frac{11}{4};\ z_8 = \frac{11}{4}\beta_1;\ z_9 = \frac{25}{4} \tag{B.29}$$

In order to solve Eqn (B.27) the first four derivatives of F_1 are required as initial condition. The following is the procedure to obtaine the initial conditions.

The Initial Conditions

Substitute $\beta = 0$ into the derivatives of F_1 in Eqn (3.3), and get,

$$\begin{aligned} \frac{d^{2i}F_1}{d\beta^{2i}}(\mu, 0) &= 0; \\ \frac{d^{2i+1}F_1}{d\beta^{2i+1}}(\mu, 0) &= (-1)^i \int_0^\infty J_0(\lambda\sqrt{1-\mu^2})e^{-\lambda\mu}\lambda^{i+1}d\lambda; \qquad i = 0, 1, ... \end{aligned} \tag{B.30}$$

The integral expression of Eqn (B.30) can be expressed in terms of Legendre functions of the first kind with degree α [see Gradshteyn and Ryzhik (1994);Eqn. 6.624.6 and 8.752.2].

$$\int_0^\infty J_0(\lambda\sqrt{1-\mu^2})e^{-\lambda\mu}\lambda^\alpha d\lambda = \Gamma(\alpha+1)P_\alpha(\mu) \tag{B.31}$$

So Eqn (B.30) become

$$\begin{aligned} \frac{d^{2i}F_1}{d\beta^{2i}}(\mu,0) &= 0; \\ \frac{d^{2i+1}F_1}{d\beta^{2i+1}}(\mu,0) &= (-1)^i\Gamma(i+2)P_{i+1}(\mu); \qquad i=0,1,... \end{aligned} \tag{B.32}$$

with $0 < \mu \leq 1$ and $Re(i+1/2) > -\frac{3}{2}$. Gamma function on the right hand side of Eqn (B.32) can be expressed as factorial,

$$\Gamma(i+2) = (i+1)! \tag{B.33}$$

Therefore substitute Eqn (B.33) into Eqn (B.32), yield

$$\begin{aligned} \frac{d^{2i}F_1}{d\beta^{2i}}(\mu,0) &= 0; \\ \frac{d^{2i+1}F_1}{d\beta^{2i+1}}(\mu,0) &= (-1)^i(i+1)!P_{i+1}(\mu); \qquad i=0,1,... \end{aligned} \tag{B.34}$$

The expression of the Legendre polynomial which is also known as Legendre functions of the first kind while the degree is an integer, is defined as

$$P_\alpha(\mu) = \sum_{k=0}^{K}(-1)^k\mu^{\alpha-2k}\frac{(2\alpha-2k)}{2^\alpha k!(\alpha-k)!(\alpha-2k)!} \tag{B.35}$$

where $K = \alpha/2$ if α is even or $(\alpha-1)/2$ if α is odd. An alternative expression of Eqn (B.35) is obtained as [see Spiegel (1968), Eqn. 25.2]

$$P_\alpha(\mu) = \frac{1}{2^\alpha \alpha!}\frac{d^\alpha}{d\mu^\alpha}(\mu^2+1)^\alpha \tag{B.36}$$

which is often referred to as Rodrigues's Formula. Hence the first three Legendre polynomials are obtained as

$$P_0(\mu) = 1; \quad P_1(\mu) = \mu; \quad P_2(\mu) = \frac{1}{2}(3\mu^2 - 1) \tag{B.37}$$

Finally the initial condition of Eqn (B.27) are,

$$\begin{aligned} F_1(\mu,0) &= 0; \quad & \frac{dF_1}{d\beta}(\mu,0) = \mu; \\ \frac{d^2F_1}{d\beta^2}(\mu,0) &= 0; \quad & \frac{d^3F_1}{d\beta^3}(\mu,0) = -3\mu + 1 \end{aligned} \tag{B.38}$$

With the same procedure, the initial conditions of F_2 and F_3 functions can be defined respectively as,

$$\begin{aligned} F_2(\mu,0) &= 0; \quad & \frac{dF_2}{d\beta}(\mu,0) = 3\mu\sqrt{1-\mu^2}; \\ \frac{d^2F_2}{d\beta^2}(\mu,0) &= 0; \quad & \frac{d^3F_2}{d\beta^3}(\mu,0) = (3-15\mu^2)\sqrt{1-\mu^2} \end{aligned} \tag{B.39}$$

and

$$\begin{aligned} F_3(\mu,0) &= 0; \qquad \frac{dF_3}{d\beta}(\mu,0) = 1-3\mu^2; \\ \frac{d^2F_3}{d\beta^2}(\mu,0) &= 0; \qquad \frac{d^3F_3}{d\beta^3}(\mu,0) = 15\mu^3 - 9\mu \end{aligned} \tag{B.40}$$

Appendix C

Code sructure of Computation

The code sructure for the computational of hydrodynamics force of linearized floating body motion in time domain is shown in Figure C.

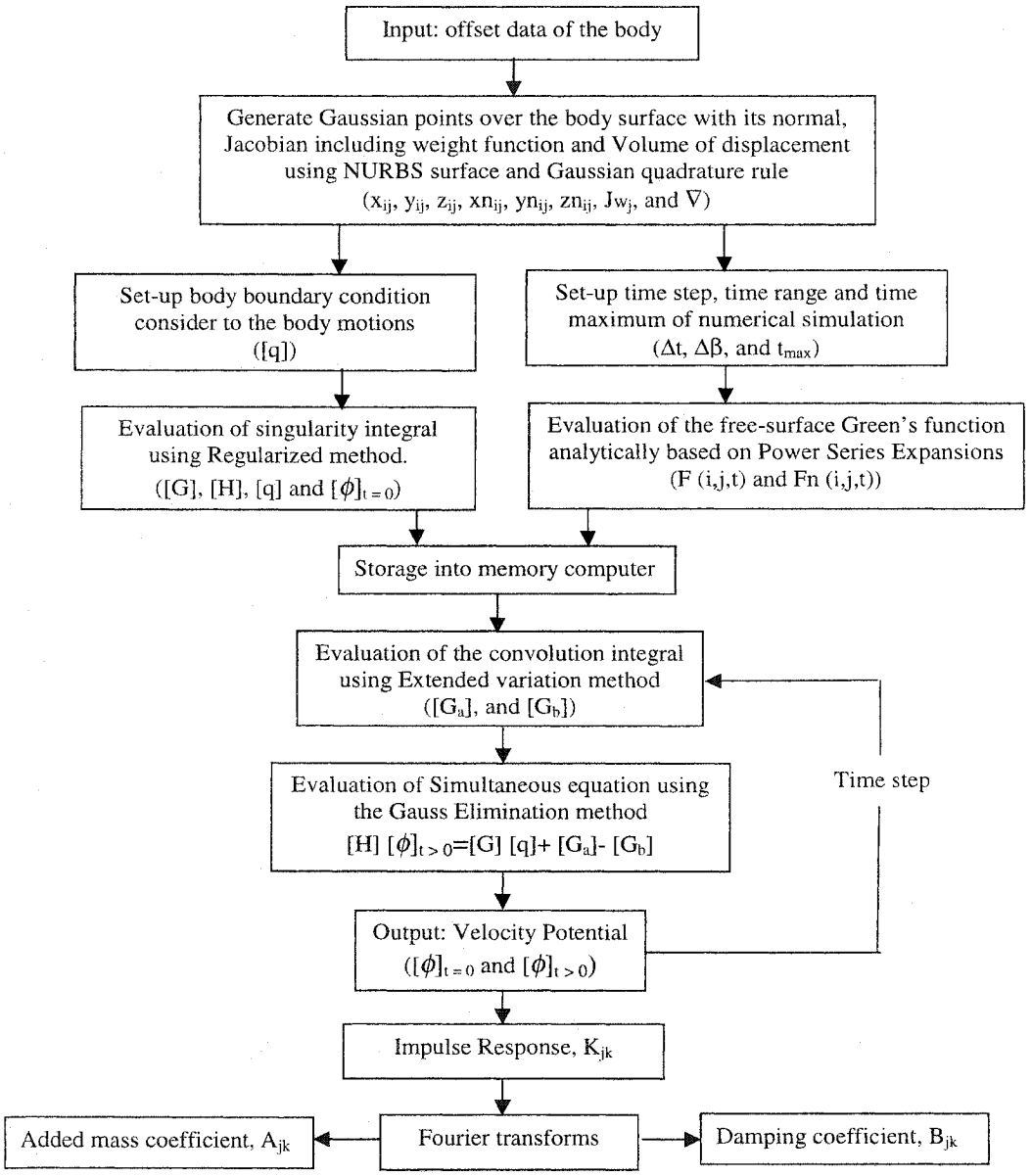

Figure C.1: Flow chart of the hydrodynamics force computation in time domain